



1 **Geospatial modelling of large wood supply to rivers: a state-of-the-**
2 **art model comparison in Swiss mountain river catchments**

3

4 Nicolas Steeb^{1,*}, Virginia Ruiz-Villanueva^{2,3}, Alexandre Badoux¹, Christian Rickli¹, Andrea
5 Mini³, Markus Stoffel^{2,4,5}, Dieter Rickenmann¹

6

7 ¹Swiss Federal Research Institute WSL, Zürcherstrasse 111, CH-8903 Birmensdorf,
8 Switzerland

9 ²C-CIA-Climate Change Impacts and Risks in the Anthropocene, Institute for Environmental
10 Sciences (ISE), University of Geneva, CH-1205 Geneva, Switzerland

11 ³Institute of Earth Surface Dynamics (IDYST), University of Lausanne, UNIL Mouline, CH-
12 1015 Lausanne, Switzerland

13 ⁴Dendrolab.ch, Department of Earth Sciences, University of Geneva, Geneva, Switzerland.

14 ⁵Department F.-A. Forel for Environmental and Aquatic Sciences, University of Geneva,
15 Geneva, Switzerland

16 *Corresponding author: Nicolas Steeb, Email: nicolas.steeb@wsl.ch

17



18 **ABSTRACT**

19 Different models have been used in science and practice to identify instream large wood
20 (LW) sources and to estimate LW supply to rivers. This contribution reviews the existing models
21 proposed in the last 35 years and compares two of the most recent GIS-based models by applying
22 them to 40 catchments in Switzerland. Both models, which we call here empirical GIS approach
23 (EGA) and Fuzzy-Logic GIS approach (FGA), consider landslides, debris flows, bank erosion,
24 and mobilization of instream wood as recruitment processes and compute volumetric estimates
25 of LW supply based on three different scenarios of process frequency and magnitude. Despite
26 being developed following similar concepts and fed with similar input data, the results from the
27 two models differ markedly. In general, estimated supply wood volumes were larger in each of
28 the scenarios when computed with the FGA and lower with the EGA models. Landslides were
29 the dominant process identified by the EGA, whereas bank erosion was the predominant process
30 according to the FGA model. These differences are discussed and results compared to available
31 observations coming from a unique database. Regardless of the limitations of these models, they
32 proved extremely useful for hazard assessment, and the design of infrastructure and other
33 management strategies.

34

35 **KEYWORDS:** large wood, GIS, modelling, landslide, bank erosion, debris flow, natural
36 hazards

37



38 1 INTRODUCTION

39 The influence of wood in watercourses is manifold. On the one hand, there are various
40 ecological benefits of large wood (LW), as it provides habitat and food source for many organic
41 organisms, thus promoting rich biodiversity (Harmon et al., 2004; Steel et al., 2003; Wondzell
42 and Bisson, 2003). LW also affects stream hydraulics by altering the channel morphology and
43 sediment control (Montgomery and Piégay, 2003; Wohl and Scott, 2016). On the other hand, large
44 quantities of LW may be mobilized during infrequent, high-magnitude floods and may induce
45 potential hazards for human settlements and infrastructure (Lucía et al., 2015c; Lucía et al., 2018;
46 Rickli et al., 2018; Ruiz-Villanueva et al., 2013; Steeb et al., 2017b). Consequently, river
47 managers are challenged to maintain a good ecological status of rivers while minimizing potential
48 hazards.

49 From a flood protection perspective, the main problem regarding LW in streams is wood
50 accumulation at bridges, and weirs, which reduces or even clogs the entire river cross section and
51 leads to backwater rise and consequent inundation (Comiti et al., 2016; Lassetre and Kondolf,
52 2012; Piégay et al., 1999; Rickenmann et al., 2016). The associated damage potential of LW
53 depends mainly on the volume of transported LW. Large wood transport is governed by the flow
54 conditions, river morphology (Ruiz-Villanueva et al., 2020), the size and shape of individual
55 wood pieces (i.e., large logs or rootwads are more prone to clogging; Bezzola et al., 2002), the
56 mode wood is being transported (i.e., if logs are transported congested or not; Braudrick et al.,
57 1997; Ruiz-Villanueva et al., 2019) and the availability or supply of wood. Wood supply occurs
58 by numerous geomorphic processes including bank erosion, channel migration, mass wasting
59 (e.g., landslides, debris flows) and natural tree mortality and fall (Benda and Sias, 2003). These
60 processes can be highly variable, both on temporal and spatial scales (Gasser et al., 2019).

61 Despite numerous existing approaches and efforts (see following section), the quantitative
62 estimation of LW supply volume and the definition of contributing source areas based on different
63 recruitment processes remain very challenging. Because LW transport happens at the end of a
64 long process cascade (precipitation as trigger, flood formation and recruitment processes as



65 supplier, channel discharge as transport medium), its estimation involves many uncertainties that
66 are difficult to quantify. In addition, any type of model developed to estimate and quantify wood
67 supply should be validated with field observations, data that is very scarce (Comiti et al., 2016;
68 Seo et al., 2010).

69 This work reviews the state-of-the-art in wood supply modelling and presents a comparison
70 of two recent GIS based approaches based on a similar general concept and using similar input
71 data. The models were validated with a unique observation dataset of supplied wood during single
72 events in a large number of catchments in Switzerland (Steeb, 2018; Steeb et al., 2019a). We
73 discuss uncertainties, limitations and strengths of the two models and compare them with other
74 recent approaches. In addition, we also consider implications for flood hazard assessment and
75 river management.

76

77 **2 LARGE WOOD SUPPLY MODELS: A REVIEW**

78 Over the last decades, different approaches have been developed to quantify LW supply at
79 both, reach and catchment scales. Gregory et al. (2003) provided a summary of the first attempts
80 to simulate wood supply, i.e., mostly mathematical models developed from conceptual
81 descriptions of selected wood recruitment processes. Later, Gasser et al. (2019) reviewed recent
82 approaches and evaluated whether the stabilizing effect of vegetation on total LW supply was
83 considered or not. Here we compile information on existing approaches and expand these
84 overviews to provide a review of published approaches to model recruitment processes and to
85 quantify LW supply (Table 1). We classify the approaches by model category (i.e., empirical,
86 deterministic, stochastic, or GIS-based) and summarize their main characteristics (i.e., processes
87 considered, spatial and temporal scales, inputs and outputs, and whether they were validated with
88 field observations or not). The evolution of these models illustrates and contributes to the
89 scientific understanding of the complex processes involved in wood supply to rivers. Some of the
90 earliest approaches (e.g., Malanson and Kupfer, 1993; Minor, 1997; Rainville et al., 1986; Van



91 Sickle and Gregory, 1990) were designed to simulate long-term delivery of wood to river reaches
92 from adjacent riparian forest by tree mortality, windthrow or bank erosion. Subsequent models
93 attempted to describe these input processes over larger portions of river networks (Beechie et al.,
94 2000; Bragg, 2000; Downs and Simon, 2001; Kennard et al., 1999; Meleason et al., 2003; Welty
95 et al., 2002), but maintained a long-term perspective. Few studies included other processes, such
96 as channel avulsion (Malanson and Kupfer, 1993; Downs and Simon, 2001). These earlier models
97 were developed in the US, most of them in the Pacific Northwest and a few in the Southeast (e.g.,
98 Downs and Simon, 2001) or the Rocky Mountains (e.g., Bragg, 2000). Later, researchers started
99 to apply and develop models elsewhere (e.g., New Zealand; Meleason et al., 2003).

100 Martin and Benda (2001) and Benda and Sias (2003) were pioneers in considering mass
101 movements (i.e., landslides and debris flows) as wood recruitment processes, and they established
102 the first conceptual framework for LW budgeting. This approach has been further applied in US
103 mountain rivers (Benda and Bigelow, 2014; Hassan et al., 2016) before it has been adapted to
104 shorter timescales for mountain rivers in Italy and Switzerland (Comiti et al., 2016; Lucía et al.,
105 2018; Steeb et al., 2017b). Focusing on shorter time windows and on episodic disturbances (e.g.,
106 floods) aggregated at the catchment scale, researchers proposed empirical equations based on
107 field observations of exported wood and catchment characteristics (Rickenmann, 1997; Rimböck,
108 2003; Steeb, 2018; Steeb et al., 2019a; Uchiogi et al., 1996). As most of the data used to derive
109 such empirical formulas originated from steep headwater streams and mountain rivers in
110 Switzerland, Austria, and Japan, application to larger catchments is associated with considerable
111 uncertainty.

112 In order to extend the analysis to larger areas, covering multiple (sub-)catchments and
113 applying a spatially distributed analysis, another group of models (i.e., geospatial models) used
114 geographic information systems (GIS) that allowed a spatially explicit assessment of different
115 LW recruitment processes, the identification of source areas and the estimation of LW volumes.
116 Rimböck (2001) developed a GIS-based model to identify potential recruitment areas of LW in
117 mountain streams, resulting from bank erosion, landslides and windthrow. In this approach, he



118 used wood volume reduction factors to distinguish between the potential LW volume (i.e.,
119 maximum volume that could potentially be supplied) and the estimated wood volume exported or
120 supplied during exceptional floods. Mazzorana et al. (2009) developed a procedure to determine
121 the relative propensity of mountain streams in Bolzano Province (Italy) to supply wood due to
122 floods, debris flows in tributaries, bank erosion and shallow landslides, based on empirical
123 indicators. Kasprak et al. (2012) used light detection and ranging (LiDAR) data to estimate tree
124 height and recruitable tree abundance throughout a watershed in US Coastal Maine, and to
125 determine the likelihood for the stream to recruit channel-spanning trees at the reach scale and
126 assess whether mass wasting or channel migration was a dominant supply mechanism. Ruiz-
127 Villanueva et al. (2014c) estimated potential LW volumes recruited from landslides, bank erosion
128 and fluvial transport during floods in the Central Mountain Range in Spain. The authors applied
129 a GIS model including multi-criteria and multi-objective assessments using fuzzy logic principles
130 together with reduction factors for predefined scenarios. The method included the analysis of the
131 hillslope-channel network connectivity and the resistance of the vegetation to be eroded. This
132 approach was recently adapted and applied to mountain catchments in Switzerland, considering
133 debris flows as supply processes as well (Ruiz-Villanueva and Stoffel, 2018), and it has been
134 further used in the present study. Also applied in Swiss mountain catchments, Steeb et al. (2017a,
135 2019b) proposed a GIS approach to model source areas of LW and to estimate potential supply
136 and exported wood volumes based on reduction factors derived from an extensive empirical
137 database of flood events with LW occurrence (Steeb, 2018; Steeb et al., 2019a, 2022). In
138 Switzerland and other countries around the Alps, some private engineering companies and
139 consultants, specialized on natural hazards, developed their own GIS-based models to estimate
140 the potential LW supply from different recruitment processes (e.g., von Glutz, 2011; Hunziker,
141 2017).

142 However, one important aspect of the above-mentioned GIS-based models (Mazzorana et
143 al., 2009; Rimböck, 2001; Ruiz-Villanueva et al., 2014c; Steeb et al., 2017a, 2019b) is that they
144 do not attempt to simulate the actual recruitment processes (e.g., landslides, debris flows, bank



145 erosion), but they used available information on areas susceptible to recruitment processes (e.g.,
146 from hazard maps, although these are usually derived from previous modelling studies) or expert-
147 based buffers. An intermediate approach was proposed by Rigon et al. (2012), who applied a
148 geostatistical bivariate analysis (weight of evidence method; Bonham-Carter et al., 1990) to
149 identify unstable areas based on weighting factors. Lucía et al. (2015a) estimated potential LW
150 recruitment in a mountain basin in Italy modelling shallow landslides with a hillslope stability
151 model (Montgomery and Dietrich, 1994) coupled to a connectivity index (Cavalli et al., 2013).
152 The approach was further developed by Franceschi et al. (2019) who used detailed forest
153 information based on a single tree extraction from LiDAR data and combined it with a 1D
154 hydraulic model to evaluate channel widening and LW downstream propagation. Cislighi et al.
155 (2018) proposed one of the first physically-based stochastic models to simulate shallow landslides
156 combined with the forest stand characteristics to estimate LW recruitment from hillslopes.
157 Similarly, Gasser et al. (2018, 2020) proposed two frameworks to model shallow landslides, and
158 geotechnical and hydraulic bank erosion applying two physically-based stochastic models
159 together with a tree detection algorithm (Dorren, 2017) to estimate LW supply. Zischg et al.
160 (2018) presented a LW recruitment model coupled to a 2D hydrodynamic model to estimate LW
161 recruitment from bank erosion in the flood influence zone of the river. In this approach, wood
162 volumes were also estimated based on a single tree detection algorithm applied to a normalized
163 digital surface model.

164



165 **Table 1: Comparison of published wood supply models. Grey: models used for comparison in**
 166 **this work**

Reference	Country	Model name	Category	Processes considered	Spatial scale	Temporal scale	Main input variables	Output
Rainville et al., 1986	USA (Pacific Northwest)	Not specified	Deterministic	Tree fall	Stream reach	between 25 and 300 years (time steps of 10 years)	Not specified	Number of wood pieces
Murphy and Koski, 1989	SE Alaska	Not specified	Deterministic	Tree fall and bank erosion	Stream reach	250 years (time steps 1 year)	Survey measurements; channel width, wood diameter, forest stand	Number of wood pieces
Van Sickle and Gregory, 1990	USA (OR)	Not specified	Stochastic	Tree fall	Stream reach	time steps of 10 years	Riparian stand density, tree height, stream length	Number of wood pieces
Malanson and Kupfer, 1993	USA	FORFLO model	Stochastic	Tree fall	Stream reach / floodplain	500 years (time steps 1 year)	Tree species, tree height, diameter, water level	Biomass
Rickenmann, 1997	Switzerland, Japan, USA	Not specified	Empirical	Wood export, (recruitment process not specified)	Catchment	Event	Catchment area, forested catchment area, stream length, forested stream length, peakflow, flood runoff and bedload volume	LW potential (instream wood), estimated LW supply volumes
Beechie et al., 2000 (based on Kennard et al., 1999)	USA (WA)	Riparian-in-a-Box	Deterministic	Natural tree mortality, windthrow, bank erosion	Stream reach	150 years (time steps 10 years)	Tree species, diameter, height, and crown ratio in stands; site/reach geometry	Number of wood pieces and LW volume
Bragg, 2000	USA (Intermountain West)	CWD model (1.2)	Stochastic	Episodic tree mortality (spruce beetle outbreak, moderately intense fire, and clear-cut)	Stream reach	300 years (time steps 10 years)	Stand density, species, tree height & diameter	Number of wood pieces and LW volume
Downs and Simon, 2001 (based on earlier models of Simon, 1989 and Hupp and Simon, 1991)	USA (MS)	Simon channel evolution model	Deterministic	Bank erosion and channel avulsion	Stream reach / river network	time steps of 10 years	Channel morphology surveys, rates of knickpoint migration, quantitative characteristics of riparian vegetation	Number of wood pieces and LW volume
Rimböck, 2001	Germany (Bavarian Alps)	<i>Luftbildbasierte Abschätzung des Schwemmholtzpotenzials</i>	Deterministic GIS-based	Bank erosion, mass	Stream reach	Event	DTM, stand density	LW potential volume



		<i>LASP</i> (aerial photo-based estimation of wood potential volume)		failures (i.e., landslides), windthrow, avalanches				
Welty et al., 2002 (same model as Kennard et al., 1999 and Beechie et al., 2000)	USA (Pacific Northwest)	Riparian aquatic interaction simulator RAIS	Deterministic	Natural tree mortality, windthrow, bank erosion, mass failures	Stream reach	240 years (time steps 10 years)	Various variables describing forest stand, stream width, initial LW, conifer/hardwood depletion rate, zone widths, windthrow rate, fall direction bias, LW placement option	Number of wood pieces and LW volume
Benda and Sias, 2003	USA (Pacific Northwest)	Not specified	Deterministic	Episodic tree mortality (e.g., fire, wind), bank erosion, mass failures and debris flows	Catchment and stream reach	800-1800 years (time steps 10 years)	Stand density, tree height, channel width, recruitment area & rates	Number of wood pieces and LW volume
Meleason et al., 2003	USA (Pacific Northwest)	Streamwood	Stochastic	Tree fall by natural mortality	Stream reach	500 years (time steps 10 years)	List of trees that died in a year (wood model input = forest model output)	Number of wood pieces and LW volume
Benda et al., 2007	USA	NetMap	Deterministic GIS-based	Hillslope erosion, sediment and wood supply	Watershed, subbasin, or stream segment	Not specified	Base terrain parameters including DEM and climate data	LW accumulation type
Mazzorana et al., 2009	Italy (Autonomous Province of Bolzano)	Not specified	Deterministic GIS-based	Bank erosion, mass failures and debris flows	Catchment	Event	DTM, hazard index map (debris flow, overbank sedimentation), land use map, stand map, torrent network map	Hazard index maps classifying torrent catchments according to propensity to entrain and deliver woody material.
Eaton et al., 2012	British Columbia	The reach-scale channel simulator (RSCS) was	Stochastic (Monte Carlo)	Tree fall by natural mortality	Stream reach	One year time step	Tree height, tree diameter, tree fall orientation, forest density, chronic mortality, decay and breakage	Wood load (m ³ ·m ⁻²) and jam formation
Kasprak et al., 2012	USA (ME)	Not specified	Deterministic	Bank erosion, mass failures and debris flows	Both stream reach and catchment	100 years period	Stand data, LiDAR DEM	Number of wood pieces
Rigon et al., 2012	Italy (Eastern Alps)	Not specified	Geostatistical, GIS-based	Mass failures (i.e., landslides)	Both stream reach and catchment	Event	Landslide and debris flow inventory data, stand data, DEM	LW volume



Benda and Bigelow, 2014 (same model as Benda and Sias, 2003)	USA (CA)	Not specified	Deterministic	Tree mortality, bank erosion, mass failures, debris flows and snow avalanches	Both stream reach and catchment	100 years period	Survey measurements	Quantification of wood recruitment, storage and transport
Ruiz-Villanueva et al., 2014c	Spain	Not specified	Fuzzy-logic GIS-based	Fluvial transport, bank erosion and mass failures (i.e., landslides)	Catchment	Event	DEM, topography, natural hazards maps, geomorphological units, forest density, tree species, height & diameter	Number of wood pieces, LW volume
Lucía et al., 2015a	Italy (North-western Apennines)	Not specified	Deterministic GIS-based	Bank erosion, mass failures	Catchment	Event	DTM, DSM (digital surface model)	LW volume
Benda et al., 2016 (sensu Benda and Sias 2003)	USA (OR)	Reach Scale Wood Model (RSWM)	Deterministic	Tree fall by natural mortality	Stream reach	100 years (5-year time steps)	Stand density, mortality rate, tree height & diameter, slope, stream width	Instream wood quantity (pieces and volume)
Hassan et al., 2016 (budget concept used in Benda and Sias 2003)	Canada (BC)	Not specified	Deterministic	Tree mortality, bank erosion, mass failures	Stream reach	100 years period	High field data requirements, most can be obtained from air photo measurements, forest inventory data, and/or regional values	LW volume
Steeb et al., 2017b; Steeb, 2018 (updated and expanded from Rickenmann, 1997)	Switzerland, Italy, France, Germany Japan	Not specified	Deterministic, Empirical	Wood export, (recruitment process not specified)	Catchment	Event	Catchment characteristics, flood event characteristics	LW volume
Steeb et al., 2017a, 2019b	Switzerland (Alps)	Empirical GIS Approach (EGA)	Deterministic GIS-based, empirical	Bank erosion, mass failures, debris flows	Catchment	Event	SilvaProtect-CH data, stream network, catchment area, ecomorphology data, stand data (NFI)	LW volume, number of wood pieces, recruitment areas, proportion of fresh and dead wood
Cislaghi et al., 2018	Italy (Eastern Alps)	Combination of the probabilistic multidimensional stability model PRIMULA and a hillslope-channel transfer mode	Stochastic	Mass failures (i.e., landslides)	Catchment	Event	DEM, geological map, rainfall, forest stand characteristics	LW volume
Gasser et al., 2018 and 2020	Switzerland	SlideforMAP, BankforMAP, FINT	Stochastic	Bank erosion,	Stream reach	Event	DTM, DSM, precipitation maps, soil map,	LW volume



				mass failures			vegetation efficiency (erosion prevention)	
Ruiz-Villanueva and Stoffel, 2018	Switzerland	Fuzzy-Logic large wood recruitment Toolbox (here Fuzzy-logic GIS Approach; FGA)	Fuzzy-logic GIS-based,	Bank erosion, mass failures, debris flows	Catchment	Event	SilvaProtect-CH data, stream network, catchment area, DEM, ecomorphology data, stand data (NFI)	LW volume, recruitment areas
Zischg et al., 2018	Switzerland	LWsimR (coupled with Basement-ETH)	Deterministic	Bank erosion	Stream reach	Event	DEM, hydrograph, forest stand	LW volume
Franceschi et al., 2019 (based on the model developed by Lucia et al. 2015)	Italy (South Tyrol)	Not specified	Deterministic GIS-based	Bank erosion, mass failures	Catchment	Event	DTM, geomorphological map, precipitation, discharge	LW volume

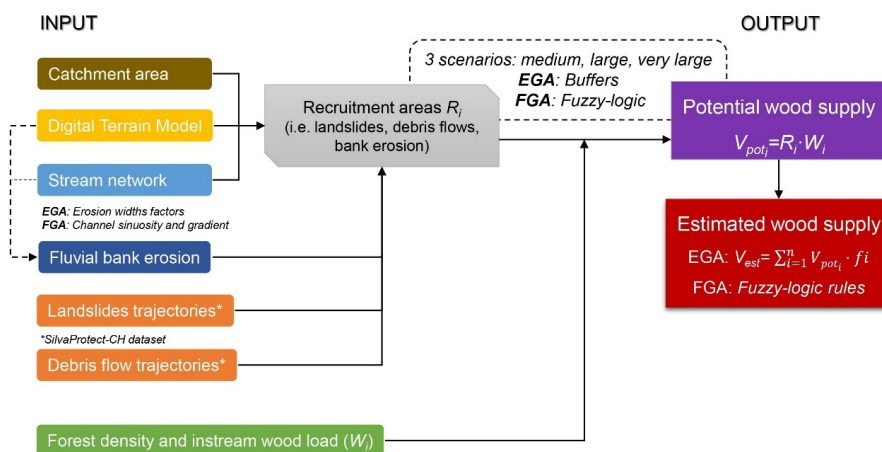
167



168 **3 GEOSPATIAL MODELLING OF LARGE WOOD SUPPLY IN**
 169 **SWISS MOUNTAIN CATCHMENTS**

170 **3.1 General concept**

171 In this contribution, two LW models were compared; the empirical GIS approach (EGA)
 172 by Steeb et al. (2017a, 2019b) and the Fuzzy-Logic GIS approach (FGA) by Ruiz-Villanueva and
 173 Stoffel (2018) which is a variation of the model presented by Ruiz-Villanueva et al. (2014c). Both,
 174 the EGA and FGA are based on a similar general concept (Figure 1) and fed with similar input
 175 data and defined equivalent scenarios (see following subsections) to make comparison possible.
 176 Both models were developed in the context of *WoodFlow*, a Swiss research program aimed at
 177 creating knowledge and methods to analyze instream wood dynamics, with particular attention to
 178 watercourses in the Alpine region (FOEN, 2019).



179

180 **Figure 1: Conceptual model of the empirical GIS approach (EGA) and the Fuzzy-Logic GIS**
 181 **approach (FGA). V_{pot} = potential wood supply [m^3]; V_{est} = estimated supplied wood [m^3];**
 182 **i = recruitment process[-]; R = recruitment area [ha]; W = forest density or instream wood load**
 183 **[$\text{m}^3 \text{ ha}^{-1}$]; f = volume reduction factor [-].**

184

185 The general concepts and main steps of the GIS-based approaches were to (i) identify the
 186 recruitment areas on the hillslopes and along the stream network that may contribute woody
 187 material to streams, such as areas affected by landslides, debris flows and bank erosion; (ii) create



188 three different scenarios based on the process frequency and magnitude; and to (iii) provide
189 estimates of potential LW supply V_{pot} (i.e., worst case scenarios) and supplied wood volumes for
190 each scenario V_{est} . The methods aim at estimating supply wood volumes at the catchment scale
191 and do not include the analysis of wood transfer (i.e., transport and deposition) through the stream
192 network.

193 Potential large wood supply V_{pot} was calculated by intersection of the modelled recruitment
194 areas with forest cover. During a flood, however, only a part of the LW potential is actually
195 recruited and exported out of the catchment. Therefore, empirically derived volume reduction
196 factors (EGA) or fuzzy logic principles (FGA) were applied to best estimate actual supplied LW
197 volumes V_{est} . Modelling results were validated by comparison with available empirical data
198 documented after flood events (Table S1 in supplementary material).

199

200 **3.2 Input data**

201 *3.2.1 Catchment areas and stream network*

202 The topographical catchment areas (feature polygons), which define the perimeters of
203 investigation, were available from the geodataset “topographical catchments of Swiss
204 waterbodies” (FOEN, 2015). The stream network of Switzerland at a scale of 1:25,000
205 (swissTLM3D, © 2016 swisstopo [DV033594]) was pre-processed by adding information on
206 channel width as derived from a Swiss-wide ecomorphological dataset (Ökomorphologie
207 Stufe F ©FOEN; Zeh Weissmann et al., 2009). Based on this dataset, the channel width was
208 known for 42 % (25,800 km) of the total Swiss streams’ length. For the remaining 58 %, we
209 extrapolated channel width based on stream order (Strahler, 1957) and altitude classes (Table S2).

210 The stream network and channel widths were used to define intersections and connectivity
211 between the hillslopes processes and the streams, to estimate the bank erosion prone areas
212 (sections 3.3 and 3.4) and to assign values of instream dead wood volumes (section 3.2.3).

213



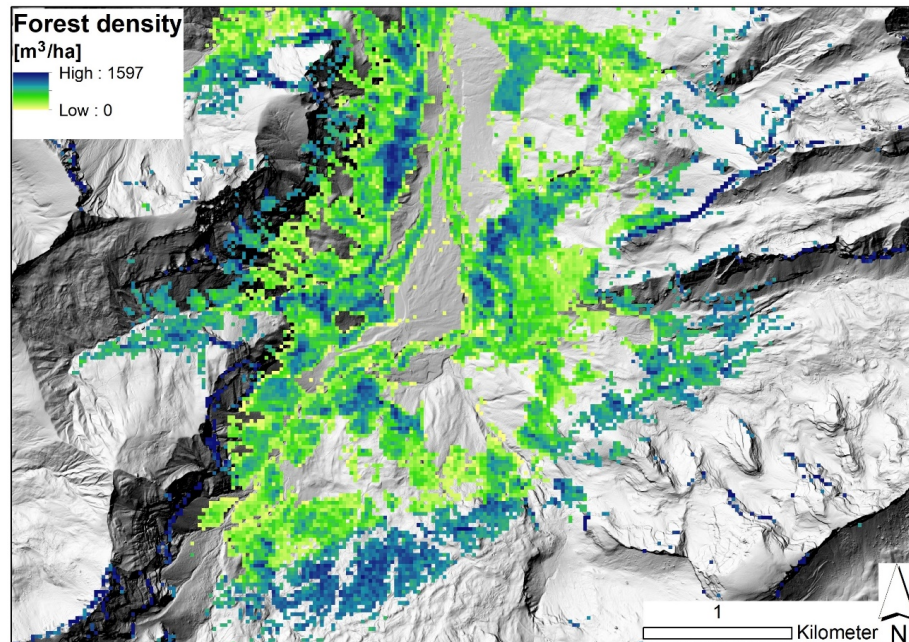
214 *3.2.2 SilvaProtect-CH and the identification of landslide and debris flow*
215 *trajectories*

216 For the modelling of the two recruitment process categories landslide and debris flow, both
217 GIS models used the SilvaProtect-CH dataset from Losey and Wehrli (2013). As part of the
218 SilvaProtect-CH project, several natural hazard processes were modelled over the entire Swiss
219 territory using partly physically-based models. As a result, process trajectories that describe the
220 topographic flow path and runout distances (from starting to deposition zone) of the investigated
221 natural hazard processes were readily available (details are provided in the supplementary
222 material). These trajectories were processed further to identify potential recruitment areas of LW
223 supply (sections 3.3. and 3.4).

224

225 *3.2.3 Forest density and instream wood load*

226 The density of living trees in Swiss forests [$\text{m}^3 \text{ha}^{-1}$] was derived from a Swiss nationwide
227 raster map with an original resolution of $25 \times 25 \text{ m}$ (rescaled to $1 \times 1 \text{ m}$; Figure 2). The raster map
228 is based on a growing stock model developed by Ginzler et al. (2019) that quantifies forest density
229 in relation to tree height (based on airborne stereo imagery), canopy cover, topographic position
230 index, mean summer temperature and elevation. The EGA and FGA models further consider an
231 estimate of deadwood on the forest floor [$\text{m}^3 \text{ha}^{-1}$] (i.e., equal to 5% of living trees density) based
232 on empirical data of the Swiss National Forest Inventory (NFI; WSL, 2016).



233
234
235
236

Figure 2: Snapshot of the wood stock raster map in the Grosse Melchaa catchment near Stöckalp (Canton Obwalden). Background: Digital terrain model (hillshade), © swisstopo.

237 Additionally, instream wood loads were included in the calculations, accounting for
238 potential LW volumes from accumulated deadwood in the channel. Detailed information on wood
239 loads across the stream network was not available, so based on a literature review by Rickli and
240 Bucher (2006) and Ruiz-Villanueva et al. (2016), volumes of instream wood were assigned to the
241 different streams grouped by channel width (EGA) or by stream order (FGA) classes (see
242 following sections).

243



244 **3.3 The empirical GIS approach (EGA)**

245 Debris flow and landslide trajectories from SilvaProtect-CH were constrained by
246 intersection with the stream network and forest cover. Only landslide trajectories with starting
247 points within a 50-m distance from the stream network were considered. This limitation was
248 supported by the landslide database of Rickli et al. (2016) where 44 % of all documented
249 landslides showed a runout distance of less than 50 m (around 80 % are within a distance of
250 100 m). For each scenario (section 3.5), different buffer widths w_b were applied on both sides of
251 the relevant debris flow and landslide trajectories (i.e., medium scenario: $w_b = 5$ m; large scenario:
252 $w_b = 10$ m; very large scenario: $w_b = 15$ m). The buffer widths were chosen in ranges according
253 to the Swiss landslide database (Rickli et al., 2016). Potential recruitment areas were finally
254 extracted as the overlap of the buffered trajectories with the forest layer.

255 The extent of bank erosion in EGA was assumed to be proportional to the given channel
256 width. Scenario-specific erosion width factors e_w (i.e., a multiple of the channel width) were
257 empirically derived from observations after the well-documented August 2005 flood in
258 Switzerland, for which a large dataset was analysed and made available (Bachmann Walker, 2012;
259 Hunzinger and Durrer, 2008). Scenario-specific erosion width factors were $e_w = 1.5$ for the
260 medium scenario, $e_w = 3$ for the large scenario, and $e_w = 4.5$ for the very large scenario. The
261 resulting buffer widths were added to the original channel width. Potential recruitment areas due
262 to bank erosion were finally extracted as the overlap of the buffered stream network with the
263 forest layer.

264 The estimation of previously stored wood load within the river network (i.e., instream
265 deadwood) was based on empirical values of wood storage per stream hectare. Rickli et al. (2018)
266 documented instream wood storage for ten reaches in Swiss torrents. This database was
267 complemented with 39 additional values from various other European rivers, based on a literature
268 review by Ruiz-Villanueva et al. (2016), in order to have reliable derivations. Finally, we assigned
269 wood load values into three channel width classes (i.e., <5 m = $94 \text{ m}^3 \cdot \text{ha}^{-1}$; 5-10 m = $67 \text{ m}^3 \cdot \text{ha}^{-1}$;
270 >10 m = $42 \text{ m}^3 \cdot \text{ha}^{-1}$).



271 Potential source areas from different recruitment processes may partly overlap. For this
272 reason, a priority sequence was determined so that such overlapping areas were not counted more
273 than once. This was defined according to the following principle: The closer to the channel a
274 recruitment process occurs, the higher the priority: instream wood > debris flow > bank erosion
275 > landslide. For example, overlapping areas of debris flows and bank erosion were assigned to
276 the process area debris flow.

277 Potential recruitment areas were finally used to calculate the potential LW supply V_{pot} by
278 multiplying the process areas with the respective forest density (for debris flows, landslides and
279 bank erosion) or wood load (for instream deadwood). From the resulting potential LW supply,
280 the actual LW supply V_{est} was estimated. To do so, volume reduction factors f were used, which
281 assumed different values depending on the recruitment process and scenario of process magnitude
282 (Table 2). The volume reduction factors were empirically determined with three different
283 approaches (Steeb et al., 2019b): 1) Comparison with literature data, including values from other
284 studies and models that proposed reduction factors; 2) comparison of potential vs. observed
285 recruitment areas; and 3) comparison of estimated vs. observed wood volumes from previous
286 floods (see the five blue catchments in Figure 3).

287 Values of observed LW supply volumes and recruitment areas together with the associated
288 catchment and flood specific parameters were taken from a complementary empirical dataset that
289 was also part of the WoodFlow research program. In total, the LW database consisted of 210 data
290 entries. Most entries (171) refer to events in Switzerland. Also included are flood events from
291 Japan, Italy, Germany and France (Steeb et al., 2019a).

292



293 **Table 2: Overview of volume reduction factors f , classified by scenario and recruitment**
294 **processes.**

Scenario	Instream wood	Debris flow	Bank erosion	Landslide
Medium	0.10	0.05	0.05	0.01
Large	0.30	0.10	0.10	0.05
Very large	0.70	0.30	0.20	0.10

295

296 The EGA model has been originally developed with ArcGIS 10.1 (©ESRI) and updated
297 with ArcGIS 10.8 (©ESRI). The toolbox is freely available for download on the website
298 www.woodflow.ch.

299

300 **3.4 The Fuzzy-Logic GIS approach (FGA)**

301 The areas prone to landslides and debris flows were defined based on the linear trajectories
302 provided by the SilvaProtect-CH database. To transform these lines into areas (i.e., pixels, as the
303 FGA is entirely raster based), the density of the lines was used to classify the terrain into three
304 intensity scenarios (section 3.5). High trajectory density was assumed to represent areas that are
305 more prone to landslides or debris flows, more likely of a higher frequency and therefore, lower
306 magnitude. Low trajectory density was assumed to represent areas that are less prone to mass
307 movements, more likely affected by higher magnitude and thus lower frequency events. The
308 thresholds to classify the three areas was based on four natural breaks (Figure S1A in
309 supplementary material). In the case of mass movements, the delivery of wood to the stream
310 network depends not only on the area of the landslide, but also on its connectivity to the channel
311 (Ruiz-Villanueva et al., 2014c). Once the trajectories were converted to density pixels, the
312 connectivity between these pixels and the stream network was established for landslide-prone
313 pixels, as a function of both the distance to the channel and the terrain slope. In addition, a buffer
314 area of influence was also established around these areas, to include toppled trees that may be



315 recruited indirectly by the action of landslides. Trees located in a landslide-prone pixel or in the
316 toppling influence area (defined as a buffer equal two times the mean tree high), may reach the
317 channel if they were close enough (Euclidean distance < 50 m) or further away but on a steep
318 slope (>40%). In the case of debris flows, all pixels were assumed to be connected to the stream
319 network.

320 Areas prone to bank erosion were computed based on channel sinuosity and gradient (as
321 proxies for channel lateral migration and transport capacity; Ruiz-Villanueva et al., 2014c), the
322 channel width and a defined width ratio. The width ratio was used to estimate the potential
323 resulting channel width after bank erosion during floods. It was calculated analysing an European
324 database (Ruiz-Villanueva et al., *in prep.*), including several rivers and flood events in
325 Switzerland and other 6 countries, and three scenarios were defined for different channel width
326 classes (9 classes ranging from < 3 to > 50 m). The stream network provided by the
327 ecomorphology database (section 3.2.1) was grouped by the channel width classes considered and
328 the width ratio was assigned to estimate the resulting potential erodible width for each stream
329 segment (Figure S1). The width ratio (ranging between 1 and 4) generally increases with scenario
330 intensity and decreasing channel width. The resulting buffers were transformed to pixels and the
331 final pixels prone to bank erosion were assigned based on channel sinuosity and gradient. Stream
332 segments characterized with high sinuosity and high gradient were assumed to be more prone to
333 bank erosion.

334 The described variables (i.e., landslide prone areas, connectivity, debris flow prone areas,
335 bank erosion prone areas, sinuosity and gradient) were transformed to fuzzy sets using the Fuzzy
336 Membership tool initially developed in ArcGIS 10.1 and updated to ArcGIS 10.7 (©ESRI) with
337 a linear membership function. The resulting converted fuzzy variables were combined (e.g.,
338 landslides prone pixels and connectivity; sinuosity and gradient) with the Fuzzy Overlay tool
339 (©ESRI). As a result, all pixels were transformed to fuzzy values ranging from 0 to 1; they were
340 then used to compute the volume of wood by multiplying the fuzzy pixel value by the forest
341 density pixel value (section 3.2.3). In case of overlapping pixels, priority was given to areas prone



342 to debris flows, then bank erosion and finally landslides (as in the EGA approach). The final
343 calculation considered also the accumulated wood load within the river network, but applying a
344 slightly different approach than for the EGA. This was estimated by assigning wood load values
345 based on literature (Ruiz-Villanueva et al., 2016) to the different river segments grouped by
346 stream order classes (i.e., < 3 stream order: $60 \text{ m}^3 \cdot \text{ha}^{-1}$; between 3 and 6 order: $120 \text{ m}^3 \cdot \text{ha}^{-1}$; > 6
347 order: $50 \text{ m}^3 \cdot \text{ha}^{-1}$) and multiplied by fuzzy layers.

348 **3.5 Model scenarios definition**

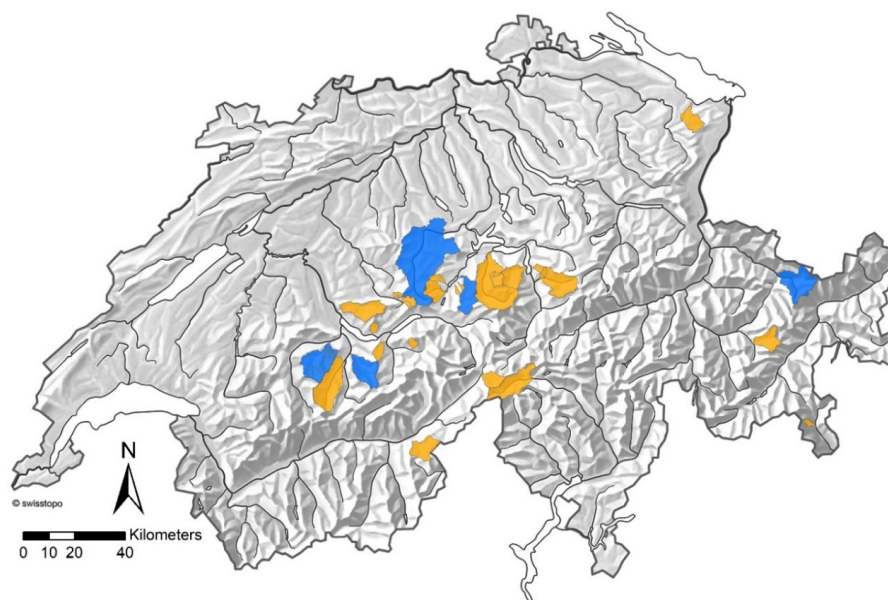
349 Three different scenarios were designed to estimate supplied wood volumes, based on a
350 qualitative assessment of the frequency and intensity of the wood recruitment processes involved.
351 These scenarios are called: medium scenario (medium-to-high frequency and intermediate
352 magnitude), large scenario (relatively low frequency and medium-to-high magnitude), and very
353 large scenario (very low frequency and very high magnitude)

354 Most of the documented floods with LW occurrence that were used to validate the GIS
355 models had a precipitation and/or peak runoff return period of 50-150 years, which was assigned
356 to the large volume scenario. The other two scenarios refer to approximate return periods and
357 were determined using *ad hoc* volume reduction factors (EGA) or the fuzzy logic rules (FGA),
358 because they could not be quantified more precisely due to a lack of data.

359 In addition to the estimated supplied wood volumes for each scenario, a potential wood
360 volume was also computed. The potential volume was assumed to be the maximum wood volume
361 supplied at the catchment scale, computed without any reduction by a coefficient (EGA) or by the
362 fuzzy logic values (FGA).

363 **3.6 Test catchments**

364 In the 40 catchments analysed in this work (Figure 3), considerable amounts of LW were
365 recruited and transported during past floods, and the resulting LW volumes were well documented
366 (mainly from the August 2005 flood; Rickli et al. 2018 and Steeb et al., 2017b). Table S1 in the
367 supplementary material provides an overview of the 40 test catchments and their characteristics.



368

369 **Figure 3: Location of the 40 test catchments (orange; with many nested sub-catchments). The**
370 **five catchments in blue (Chiene, Chirel, Grosse Melchaa, Landquart, Kleine Emme) were used to**
371 **calibrate the volume reduction factors from the EGA approach so that the estimated supplied wood**
372 **was in the same order of magnitude as the observed values from past flood events.**

373

374 **3.7. Model results analysis**

375 Model results were first compared to observed wood volumes during floods, and then
376 analysed in terms of (modelled) wood volumes per scenario, potential wood volume, wood
377 volume supplied by different recruitment or supply processes (i.e., landslides, debris flows and
378 bank erosion), and the estimated instream wood volume.

379 Statistical analyses were realized with the software RStudioVersion 2021.9.0.351 (R Studio
380 Team, 2021). Differences between the two models and between them and the available
381 observations were tested by the nonparametric Wilcoxon (Mann-Whitney) or Kruskal-Wallis tests
382 for two or more groups respectively (Stats package; R Core Team, 2019). Significance was set to
383 a p value <0.05. The dependence of wood volume on catchment controlling variables was verified



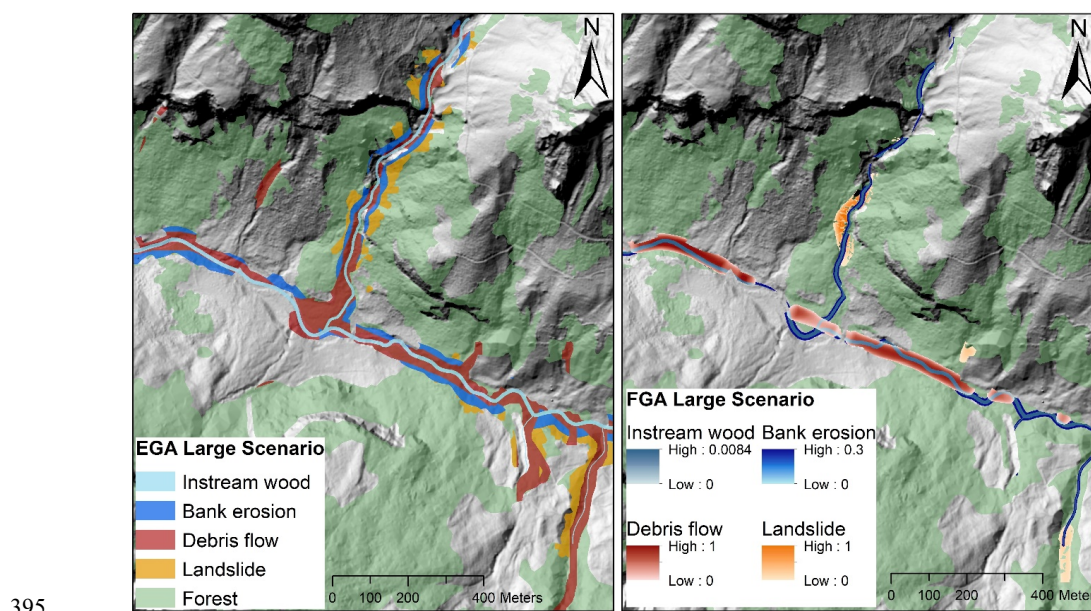
384 by means of scatter plots, regression analysis and correlation (*ggally* package; Schloerke et al.,
385 2021).

386

387 4 RESULTS

388 4.1 Comparison between model outputs and model approaches 389 (EGA/FGA)

390 The two GIS approaches provide geospatial outputs – EGA in the form of feature class
391 polygons and the FGA in pixel-based raster files – that can be visualized on a map, as shown in
392 Figure 4. Potential recruitment areas for debris flow, landslide and bank erosion are generally
393 larger for EGA, i.e., the defined EGA buffer widths provide more supply-prone areas than the
394 respective combination of FGA fuzzy layers within the same perimeter.

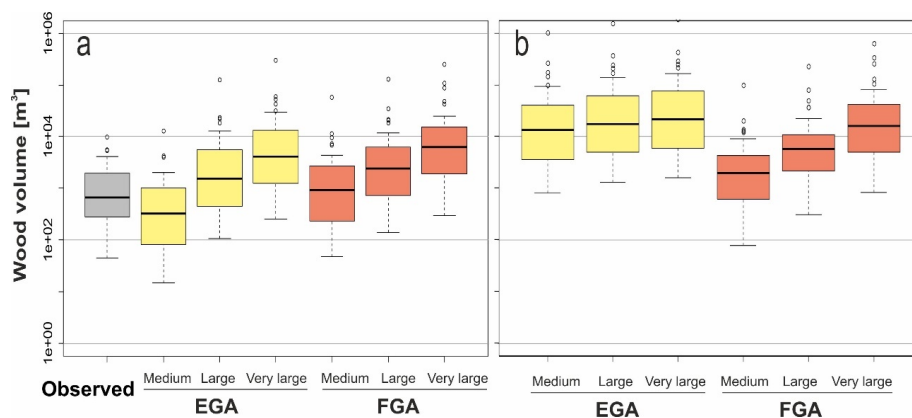


395

396 **Figure 4: Large volume scenario comparison of model outputs from EGA (left) and FGA (right)**
397 **at the Spiggebach torrent within the Chiene river catchment (Canton Bern). Potential recruitment**
398 **areas are shown for landslides (orange), debris flows (red), and bank erosion (dark blue). The stream**
399 **network (light blue) includes also instream wood loads. Background: Digital terrain model**
400 **(hillshade), © swisstopo.**



401 The estimated supply and potential wood volumes for the three scenarios and the two models
402 are shown in Figure 5 together with the available observations. The comparison between modelled
403 and observed wood volumes is presented in section 4.3, the focus here is on differences between
404 the two models. In general terms, Figure 5a highlights that the estimated supply wood volumes
405 for each scenario were larger when computed by the FGA and lower by the EGA. For example,
406 for the medium scenario, the averaged wood volumes were 994 m³ and 3318 m³ for EGA and
407 FGA, respectively. The differences were slightly reduced for the other two scenarios, for which
408 volumes equal to 7127 m³, 17353 m³, 8199 m³ and 19712 m³ were obtained (for the large and
409 very large scenarios and the EGA and FGA, respectively; Table 3).



410

411 **Figure 5: Boxplots of wood supply (a) and potential (b) volume (m³) estimated by the two models**
412 **EGA and FGA, and the three scenarios (i.e., medium, large, very large). Observed LW supply during**
413 **past events for all studied catchments (n=40) is given in grey color in panel (a).**

414



415 **Table 3: Observed and estimated LW supply volumes for the three scenarios (i.e., medium,**
 416 **large, and very large) and the two models (i.e., EGA and FGA) for all studied catchments.**

Wood supply volume [m ³]	Observed	EGA			FGA		
		Medium	Large	Very large	Medium	Large	Very large
Min.	45	15	106	253	48	141	300
1st	290	83	475	1378	244	764	2037
Median	673	329	1562	4189	921	2430	6342
Mean	1428	994	7127	17353	3318	8199	19712
3rd	1906	967	5161	12609	2588	6083	15191
Max.	9741	12757	126648	296893	57152	128575	249256

417

418 Significantly higher values were computed for the large and very large scenarios compared
 419 to the medium scenarios, with a similar pattern shown by the two models. Larger differences were
 420 observed when comparing the estimated potential volumes (Figure 5b and Table 4). In this case
 421 the EGA resulted in much higher values than the FGA (especially for medium and large
 422 scenarios), which is a result of much larger potential recruitment areas (Figure 4). Figure S3 shows
 423 that for EGA, the estimated LW supply volume corresponds to 8 % of the potential wood supply
 424 volume on average. In the case of FGA, this ratio varies much more with an average of 47 %.

425

426 **Table 4: Potential LW supply volumes for the three scenarios (i.e., medium, large, and very**
 427 **large) and the two models (i.e., EGA and FGA) for all studied catchments.**

Potential wood volume [m ³]	EGA			FGA		
	Medium	Large	Very large	Medium	Large	Very large
Min.	807	1289	1601	76	305	811
1st	3529	4949	6000	613	2203	5341
Median	13226	17579	21619	1965	5774	15965
Mean	58664	86984	105723	5961	16173	52995
3rd	37672	59612	74948	4207	10665	41066
Max.	1011306	1534850	1866295	100165	231336	632151

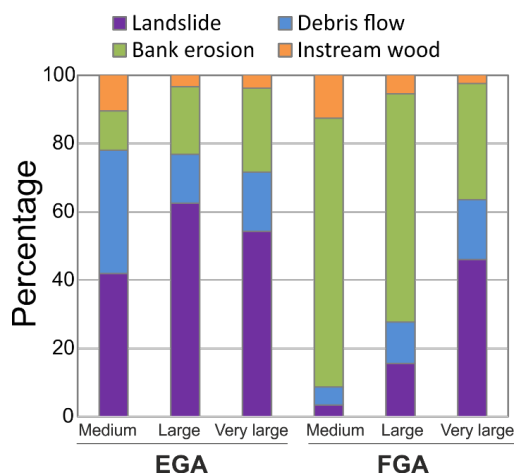
428

429



430 **4.2 Contribution from different supply processes**

431 The main difference between the two models was the estimated contribution from each
432 supply process to the obtained wood volume. Landslides were the dominant process in the case
433 of the EGA, with a contribution up to more than 60% of the computed wood volume (for the large
434 scenario); whereas bank erosion was the predominant process in the FGA model for all scenarios
435 (Figure 6). Debris flows played an intermediate role in supplying wood according to the two
436 models; however, the importance of this process varied depending on the scenario. For the
437 medium scenario, the EGA model showed a similar percentage of averaged wood supplied by
438 landslides and debris flows. The FGA, contrastingly, computed most of the averaged wood
439 volume supplied by bank erosion, and only a low percentage of wood supplied by landslides and
440 debris flows. Only for the very large scenario, the importance of landslides, in terms of percentage
441 of supplied wood, equaled or even exceeded, the volume estimated from bank erosion with the
442 FGA.



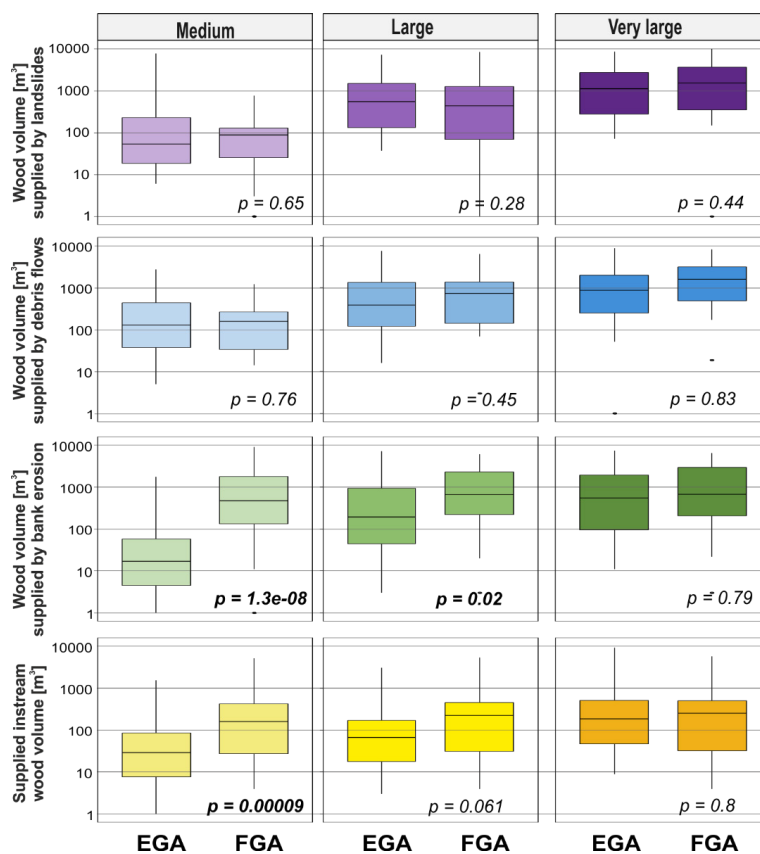
443 **Figure 6: Large wood volumes supplied by each process, model, and scenario averaged for all**
444 **40 study sites.**

445
446
447 The difference between the contribution of each process to the estimated volumes is clearly
448 shown in Figure 7 and 8 (with FGA resulting in generally higher volumes than EGA). The graph
449 illustrates that statistically significant differences were found between the computed supply wood



450 volumes by the two models and by bank erosion process. The median wood supply values (see
 451 black lines within boxplots of Figure 7) are about a factor of 1000 and 10 larger for the FGA than
 452 for the EGA, and for the medium and large scenarios respectively. This explains the relative
 453 dominance of bank erosion for the FGA (see also Figure 8), for the medium and large scenario.
 454 The wood volumes supplied by the other processes were not significantly different between the
 455 two models. Only the estimated instream wood volume for the medium scenario showed a
 456 significant difference between the EGA and the FGA, with larger volumes computed by the latter.

457



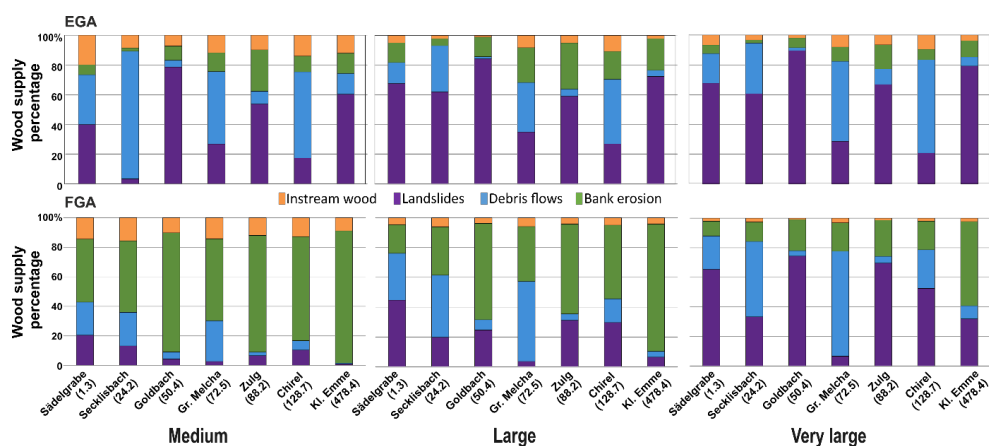
458

459 **Figure 7: Wood volumes supply estimated for landslides, debris flows, bank erosion, and**
 460 **estimated supplied instream wood by the two models and the three scenarios. The p-value is from the**
 461 **Wilcoxon test (significant values shown in bold).**



462 However, the contribution of each process to the computed wood volume did not only vary
 463 according to the model, but also according to the site. Figure 8 shows a selected sub-dataset of
 464 catchments with different drainage areas, revealing the large variability of the dominant wood
 465 supply process, and the dominance of different processes over the others in the two models. In
 466 general, the FGA approach shows a larger contribution from landslides and debris flows in smaller
 467 catchments, while landslides are the major contributor to wood supply regardless the catchment
 468 size for the EGA. Bank erosion is a minor contributor to the estimated supply in EGA for most
 469 sites and irrespective of the scenario used. However, bank erosion is the most relevant process for
 470 the FGA, which is clearly illustrated by the Kleine Emme River catchment, the largest of the study
 471 sites of the dataset, for which the FGA estimates the largest contribution by this process. The
 472 EGA model, on the other hand, estimated a larger contribution from landslides for this site.

473 The proportion of instream wood loads remains constant, independent of catchment size (2-
 474 13 % of total wood supply). The contribution of debris flows and landslides are highly variable
 475 depending on topography, and can be dominant for small (e.g., Secklisbach) or large catchments
 476 (e.g., Grosse Melchaa or Chirel).



477

478 **Figure 8: Percentage of wood volume supplied by each process, model, and scenario for selected**
 479 **studied sites, the names and catchment area in (km²) are provided in the abscissa.**

480

481 4.3 Estimated and observed wood volumes

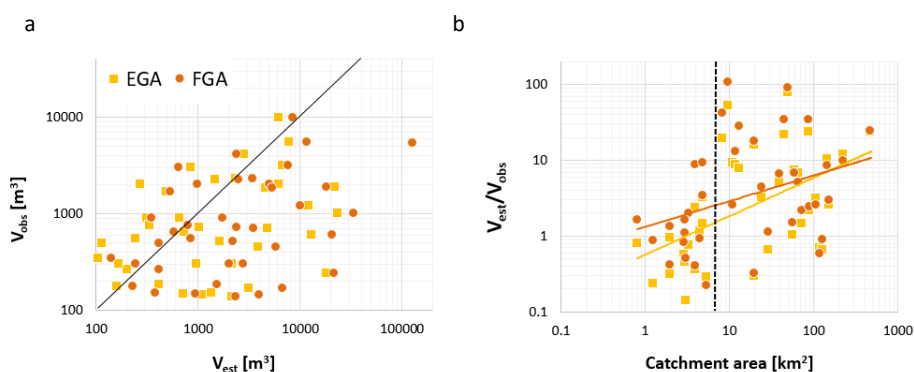
482 The comparison between observed LW volumes V_{obs} and estimated (modelled) LW volumes
 483 V_{est} are shown in Figure 9a. There is a relatively large scattering when comparing observed and
 484 estimated wood loads. Both under- and overestimation of V_{obs} are observed for both models, with
 485 a larger tendency for overestimation. Overestimation remains generally within two orders of



486 magnitude (typically higher values for FGA), underestimation within one order of magnitude
487 (typically lower values for EGA).

488 Figure 9b further shows the ratio of V_{est}/V_{obs} versus catchment area. Both under- and
489 overestimation of V_{obs} are present over >2 order of magnitude for all catchment areas. However,
490 in general, overestimation increases with increasing catchment size for both models. There is a
491 shift around a catchment area of 7 km², above which overestimation is significantly larger (with
492 a factor of >10). In catchments with areas less than 7 km², estimated wood supply is generally
493 underestimated (see dashed line in Figure 9b).

494



495

496 **Figure 9: Left: Modelled LW V_{est} (large scenario) versus observed wood volume V_{obs} during past**
497 **events. The black line shows the line of equality (1:1 line). Right: Ratio of V_{est}/V_{obs} versus catchment**
498 **area.**

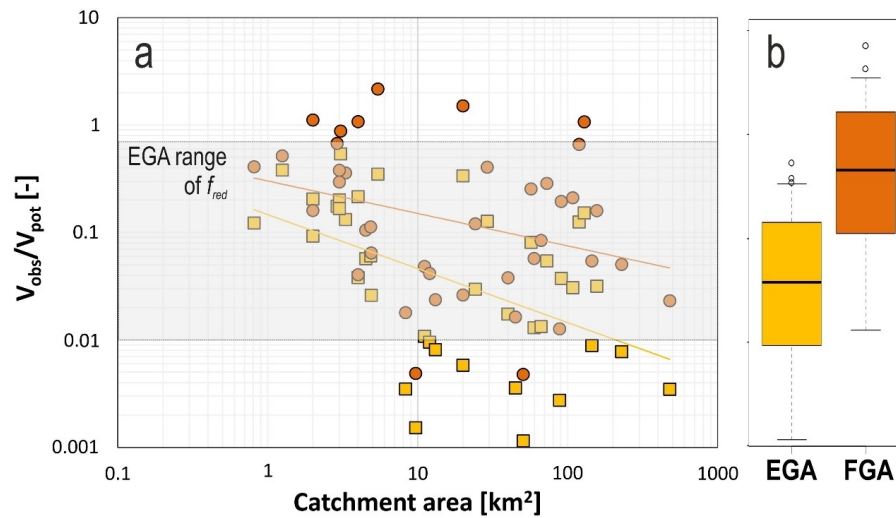
499

500 This tendency of overestimation with increasing catchment size can also be explained by
501 comparing the ratio of observed and potential wood volume V_{obs}/V_{pot} versus catchment area
502 (Figure 10a). With increasing catchment size, there is a trend of decreasing ratio values of
503 V_{obs}/V_{pot} . This means in larger catchments, the volume reduction factors (FGA) and the fuzzy rules
504 (FGA) are often not small enough to reduce the wood potential accordingly, creating
505 overestimation of wood volumes ($V_{est} > V_{obs}$).

506 Since potential wood volumes are much higher for EGA (Table 4 & Figure 5b), the ratio of
507 V_{obs}/V_{pot} is also much smaller in case of EGA (almost one order of magnitude difference as shown



508 in Figure 10b). For FGA few examples (i.e., six orange dots in Figure 10a) exist for which the
509 potential wood volume is even smaller than the observed wood volume ($V_{obs}/V_{pot} > 1$).



510

511 **Figure 10: Ratio of observed wood volumes and potential wood volumes computed by the two**
512 **models for all sites and their catchment areas. The grey rectangle shows the reduction factor**
513 **used for EGA computations.**

514



515 **5 DISCUSSION**

516 **5.1 Major differences between the two models and remaining challenges**

517 Both the EGA and FGA are based on a similar general concept, were fed with similar input
518 data (e.g., stream network, forest density, areas affected by landslides and debris flows) and run
519 with defined equivalent scenarios which made the comparison possible. However, there are also
520 some methodological differences that resulted in different model outputs. Here we describe them,
521 while in the following section we discuss our results comparing them to current knowledge and
522 other existing methodologies.

523 The most relevant difference between the EGA and FGA is the approach to define the areas
524 affected by **bank erosion**, thus the contribution of this recruitment process and the estimated
525 wood supply volumes. EGA uses buffers around the stream network computed for each scenario
526 with one specific width factor, independent of the original channel width. The resulting buffer
527 widths were added on both sides of the original channel width (section 3.3). FGA also assigned
528 scenario-specific buffers, computed with width ratios that vary according to nine channel width
529 classes (Figure S1). Half of the resulting buffer widths were added on both side of the original
530 channel width. As a result, potential bank erosion recruitment areas are generally larger for EGA
531 than for FGA. However, the reduction factors used for the EGA assumed that between 5% and
532 20% of the potential wood volume within these areas contribute to the estimated wood supply,
533 which resulted in a much lower estimated wood volume. In the case of the FGA, the entire forested
534 area identified as prone to bank erosion along the river network is contributing to wood supply
535 and the volume is reduced based on fuzzy logic pixel values (computed based on sinuosity and
536 channel slope, and going up to 30% of the potential), which resulted in a much larger volume.
537 This difference is particularly relevant for the medium scenario, for which the bank erosion width
538 identified by both models are quite similar, but the resulted wood volumes significantly differ
539 (e.g., average wood volume equal to 114 and 2613 m³ for EGA and FGA respectively for all
540 sites). This difference in the way of computing recruitment areas from bank erosion and related
541 wood volumes explains the second most important difference between the two models. As shown



542 in section 4.2, landslides are the **dominant recruitment process** in the case of the EGA, whereas
543 bank erosion is the predominant process in the FGA model. In both models, for landslides and
544 debris flows, the input data were the trajectories from the SilvaProtect-CH database, but the EGA
545 applies an expert-based buffer for each scenario to those trajectories, while the FGA groups them
546 in three classes according to their density. In addition, the fuzzy connectivity applied in the FGA
547 further reduces the areas identified as prone to mass movements (only for landslides). This
548 hillslope-channel network connectivity is another methodological difference between the two
549 models. In EGA, as a proxy for connectivity, only landslide trajectories within 50 m distance from
550 the stream network were considered. FGA considers connectivity as a function of both the
551 distance to the channel and the terrain slope (as used by Ruiz-Villanueva et al., 2014c).
552 Noteworthy, both models use Euclidean distance, but no geomorphometric measures (e.g.,
553 steepest downslope direction) as often used to assess sediment connectivity (e.g., Cavalli et al.,
554 2013).

555 The EGA generally produces much larger potential recruitment areas for landslides and
556 computes larger wood supplied by landslides than the FGA, for all three scenarios. For the FGA,
557 landslides are minor supplier of wood for the medium and large scenarios, while their contribution
558 for the very large volume scenarios significantly increases.

559 Existing observations show that mass wasting processes, such as debris flows and landslides,
560 often are the most relevant recruitment processes in smaller headwater catchments (e.g., Rigon et
561 al., 2012; Hassan et al., 2016; Seo et al., 2010). In contrast, (lateral) bank erosion is often prevalent
562 farther downstream in larger mountain or lowland rivers, resulting in large volumes of LW supply
563 by this fluvial recruitment process. This was observed after the large flood in 2005 in Switzerland
564 (Steeb et al., 2017b), the large flood in the Magra River catchment in Italy in 2011 (Lucía et al.,
565 2015c; Comiti et al., 2016) and along the Emme river catchment in 2014 (Ruiz-Villanueva et al.,
566 2018). In smaller streams, bank erosion and channel widening can also be significant, especially
567 in natural reaches (no stream regulation works), as seen after severe flash floods in Braunsbach,
568 Germany in 2016 (Lucía et al., 2018). In most of these cases, only a small proportion (<30%) of



569 the total recruited wood was supplied by mass wasting processes, and the majority of the supply
570 was due to bank erosion and channel widening along the river network.

571 Such catchment size-specific trends of dominant recruitment processes are not clearly
572 prevalent in the model results of EGA and FGA. Generally, the variability in the recruitment
573 processes and thus in the wood supply is very large, both in empirical data as well as in modelling
574 results, highlighting the importance of other catchment- and event-specific characteristics. The
575 relationship of estimated LW supply with catchment characteristics is shown in supplementary
576 material Figure S2. The highest correlation is seen for forested stream length that can be
577 interpreted as a proxy for potential supply volume for bank erosion. High correlations also exist
578 for Melton ratio and relief ratio, both surrogates for watershed slope, a factor that is directly
579 related to stream power and debris flow and landslide propensity. In general, V_{obs} from EGA
580 shows slightly higher correlations (R^2) with catchments characteristics than FGA. More research
581 is needed to better understand wood recruitment processes and to improve predictive models on
582 a physical basis. This will help to determine where and how likely mass wasting (landslides) or
583 bank erosion could occur.

584 The results in section 4.3 indicate that there is both under- and overestimation of wood supply
585 volumes. As shown in Figure S4, potential LW supply V_{pot} generally increases with catchment
586 size. During a convective storm event, often only a part of the catchment is affected, and therefore
587 geomorphologically active, so that LW supply may easily be overestimated ($V_{est} > V_{obs}$). In
588 smaller catchments and torrents, sporadic recruitment processes such as landslides or debris flows
589 can dominate and deliver large amounts of wood at once, so that wood supply may be
590 underestimated by our models ($V_{est} < V_{obs}$).

591 A less relevant difference between the models, and in terms of the total contribution to the
592 wood volume estimations, is the approach used to assign previously **deposited instream wood**
593 **loads**. The EGA assigns instream wood load values into three channel width classes (section
594 3.3), whereas FGA assigns wood load values into three stream order classes (section 3.4). The
595 main divergence comes from the assumption that the smaller channels contain the largest instream



596 wood load for the EGA (following observations in 10 small mountain streams in Switzerland
597 from Rickli et al., 2018), while the FGA assumes that larger loads are present in medium order
598 channels (as proposed by Wohl, 2017). Despite the different approaches, both models used
599 empirical data from Ruiz-Villanueva et al. (2016) to assign volumes, and the resulting wood load
600 volumes were only significantly different in the case of the medium scenario (Figure 7).

601 These differences in the methodologies result in differences in the outcomes, in terms of the
602 **potential and estimated wood supply**. The EGA generally produced larger potential recruitment
603 areas. The volume reduction factors applied in EGA are, however, on average much smaller than
604 the respective fuzzy-logic values created in FGA (Figure S3). As a result, estimated wood supply
605 is generally larger for FGA, as shown in section 4.1. For our test catchments, the application of
606 simple empirical volume reduction factors as part of the EGA model has proven to be similarly
607 accurate in estimating LW volumes, in comparison with a spatially explicit approach such as the
608 FGA model. Still, both the expert-based buffer widths and the reduction factors were defined for
609 the test catchments and validated for similar catchments located in the Alps and pre-Alps, and so
610 they should be carefully tested if applied to other rivers with different characteristics. The fuzzy
611 logic approach indirectly includes this uncertainty or imprecise information (i.e., buffer widths
612 and volume reduction factors), and allows being computed without prior existing observations or
613 knowledge. In both cases, the two models may over- or underestimate the wood volumes, but
614 allow reliable computation of wood supply volumes at the catchment scale and for three scenarios.

615

616 **5.2 Qualitative comparison of EGA and FGA with other similar** 617 **approaches**

618 As described in the introduction, just a few approaches have been proposed to compute
619 wood supply at the catchment scale considering different recruitment processes (e.g., landslides,
620 debris flows, bank erosion). As those models presented here, most frameworks, particularly those
621 based on GIS and geoprocessing (e.g., Mazzorana et al., 2009) do not attempt to simulate the
622 actual recruitment processes, but they used existing information on areas susceptible to certain



623 processes (as the EGA and FGA) from hazard maps or other sources or apply expert-based buffers
624 (as the EGA). Very few models simulate only one recruitment process (i.e., landslides or bank
625 erosion) explicitly (Lucía et al., 2015a; Cislighi et al., 2018; Zischg et al., 2018; Franceschi et al.,
626 2019; Gasser et al.; 2018, 2020). Yet, a model that simulates coupled processes to compute wood
627 supply is still lacking. In existing approaches, physically based models are combined with
628 empirical approaches to identify recruitment areas from one single process and compute wood
629 supply at the catchment scale. Still, these models require additional input data, such as
630 precipitation, discharge, soil characteristics etc., which is usually not available or challenging to
631 obtained at the desired resolution. In addition, they are much more expensive in terms of
632 computational time, which limits their application to larger areas. Therefore, there is a gap
633 between the current state-of-the-art of geomorphic process modelling and wood recruitment and
634 supply estimation.

635 Moreover, the majority of existing models used to predict wood supply are deterministic,
636 in that they do not consider the natural process variability and parameter uncertainties. Only the
637 fuzzy logic approach (Ruiz-Villanueva et al., 2014c; Ruiz-Villanueva and Stoffel, 2018)
638 indirectly considers uncertainty, but it does not represent a description of the physical supply
639 processes. A few stochastic models have been proposed (e.g., Bragg, 2000; Eaton et al., 2012;
640 Gregory et al., 2003) to simulate wood recruitment, but they were designed to work at the scale
641 of the river reach only. At the catchment scale, a probabilistic multi-dimensional approach has
642 recently been proposed (Cislighi et al., 2018) to study wood sources from hillslopes, modelling
643 areas susceptible to landslides, but it neglects other processes such as bank erosion. The latter
644 process has been considered in one of the most recent studies on LW (Gasser et al., 2020).

645 On the other hand, empirical estimation formulas (e.g., Steeb, 2018; Rickenmann, 1997;
646 Uchiogi et al., 1996) are easier and faster to apply to estimate LW supply. However, they provide
647 only an estimate for the whole catchment under investigation, without any spatial differentiation.
648 EGA and FGA, on the other hand, support a comprehensive spatial overview and direct attention
649 to areas in which a more precise assessment of the instream wood situation is necessary, e.g.,



650 through field surveys or expert assessments. Figure S5 shows that the EGA and FGA modelling
651 results approximately correspond to the 50-90% relation between V_{obs} and catchment area as
652 described with the empirical formula of Steeb (2018).

653

654 **5.3 Uncertainty in the observed and modelled LW volumes**

655 The two GIS approaches presented here yielded similar orders of magnitude of LW supply
656 for a given catchment and for the three designed scenarios. Still, several uncertainties associated
657 with the estimation of LW supply remain, and they are not just related to the obtained results and
658 the applied methodologies, but also to the available observations (coming from surveys after flood
659 events) used for calibration and validation.

660 The observed wood volumes V_{obs} were compiled mostly from technical reports of post-
661 event analyses, and these values might be in some cases only rough estimates, with a considerable
662 uncertainty. LW volumes were estimated based on LW deposits and piles in the field, for which
663 the volume and the corresponding wood content (or pore volume, respectively) must be estimated.
664 The assessment of the wood volume of such accumulations might be challenging and uncertainty
665 might be high (Spreitzer et al., 2020; Thevenet et al., 1998). Some of the observed wood volumes
666 V_{obs} were also determined on the basis of forest loss areas, for which a pre-event forest density
667 value W must be assumed. In the analysis made with the GIS models, the forest density raster
668 map of Ginzler et al. (2019) was used, which may differ from values used during the post event
669 surveys. Furthermore, the time gap between a LW transporting flood event and the survey year
670 on which the forest density map is derived from, needs to be accounted for. Depending on this
671 relationship, wood volumes may be underestimated (i.e., survey year after flood event) or
672 overestimated (i.e., survey year before flood event). This circumstance could also explain why in
673 some cases of the FGA calculations the potential wood volume is even smaller than the observed
674 wood volume ($V_{obs}/V_{pot} > 1$; see Figure 10a). This discrepancy appeared mostly in one large
675 catchment (i.e., Chirel) and its subcatchments (i.e., Fildrich, Goldbach, Rütigrabe), and could be



676 related to the forest density data used to compute the wood supply volumes, which was computed
677 with the forest after the large flood in 2005.

678 The observations we used remain a unique and extensive dataset (Steeb et al., 2019a),
679 which allowed us to parametrize the models more accurately. The EGA uses empirical volume
680 reduction factors that were derived from this dataset for the conversion of V_{pot} to V_{est} . In case of
681 debris flows, for example, the volume reduction factors f also rely on an event analysis of the
682 August 2005 flood in Switzerland by Rickenmann et al. (2008), who showed that, on average, 11-
683 19 % of all torrents in the main investigated mountain river catchments were associated with
684 debris flow activity. This percentage range was used to define the reduction factors as shown in
685 Table 2. This highlights the importance of in-depth post flood event analyses, as these provide
686 valuable empirical datasets that can be used to validate and further develop models to estimate
687 supplied LW volumes. The application of models should not replace field work surveys, but they
688 should be used in a complementary manner.

689 Another source of uncertainty is given by the SilvaProtect-CH trajectories. Since their input
690 data, in particular geology, provide a large-scale representation of natural conditions (see text in
691 the supplementary material), the SilvaProtect-CH trajectories are best suitable for use on a
692 catchment-scale range. Furthermore, SilvaProtect-CH trajectories generally result in a pessimistic
693 picture under unfavourable conditions (e.g., no consideration of the stabilizing influence of
694 vegetation cover). As a consequence, only a small part of the trajectories is expected to be active
695 during rainfall and consequent floods. In addition, the actual run-out zones of mass wasting
696 processes may often be shorter than the modelled trajectories.

697 One important limitation of the EGA and FGA models presented in this study is that the
698 available input forest cover, does not provide any further information about the forest typology,
699 structure and species composition. Despite the role that differences in forest may play in
700 stabilizing the soil and slopes and in influencing bank erosion and hillslope stability (Gasser et
701 al., 2019), the two methods do not explicitly consider this effect. Moreover, the type, structure
702 and stage of forest stand control the extent to which trees can be uprooted and recruited and



703 supplied to rivers (Mazzorana et al., 2009; Ruiz-Villanueva et al., 2014c). This aspect was
704 described as the vegetation resistance defined by Ruiz-Villanueva et al. (2014c) based on the tree
705 species and forest stage, the structural classification of forested areas made by Blaschke et al.
706 (2004) and the availability indicator used by Mazzorana et al. (2009). However, there was no
707 available information with the required spatial resolution to consider the proportion of different
708 species, the stage (e.g., remnant or reforested) or the age of the forest stand. Neglecting the
709 different response of different forest types may result in an overestimation of supplied volumes.

710 As discussed above, modelling and quantification of wood supply volumes is characterised
711 by many uncertainties. After all, the two models presented in this study allow quantifying the
712 magnitude of the expected LW supply, thus further expert judgement and knowledge of local
713 (geomorphic) characteristics is required to adequately interpret the results. The ratio between
714 predicted and observed LW volumes varies by about 1-2 order of magnitudes. For comparison it
715 is noted that a similar or even larger range of uncertainty can be expected for the estimation of
716 bedload volumes transported during floods (e.g., Rickenmann and Koschni, 2010).

717

718 **5.4 Implications for hazard assessment and river management**

719 From a practical perspective, geospatial LW modelling results can be used for hazard
720 assessment, infrastructure design, and the definition of management strategies. From a scientific
721 perspective, further applications are possible. For example, estimated wood volumes can be
722 applied as an input for a wood transport model, such as Iber-Wood (Ruiz-Villanueva et al., 2014a,
723 2014b, 2015) or other approaches (e.g., Mazzorana et al., 2011), to define realistic boundary
724 conditions. Furthermore, if no observation data are available for reference, estimated wood
725 volumes from EGA and FGA can be used to quantify blocking probabilities due to LW at bridge
726 piers or at other critical cross-section (Schalko, 2019; Schalko et al., 2018; Schmocker and
727 Weitbrecht, 2013).



728 As described in section 4.2, the average proportion of instream deadwood (instream wood
729 load) from the total potential LW supply in the 40 test catchments ranged between 2-13 % (Figure
730 6). This range is confirmed by other studies and event analyses (Dixon, 2013; Rickli et al., 2018;
731 Waldner et al., 2009). It can be concluded that instream deadwood generally accounted for only
732 a small proportion of the total LW transported during past floods in Switzerland. Rather, it is
733 freshly recruited wood that made up the majority of the transported wood volumes. Deadwood
734 alone, both on the forest floor and in the channel itself, may therefore only lead to a limited
735 increase in risk from a natural hazard management perspective. As a consequence, the artificial
736 removal of deadwood from the stream and its surroundings is not always necessary, keeping in
737 mind the ecological benefits of instream wood.

738 EGA and FGA are area-wide products that can be applied in any Swiss catchment. They
739 use a standardized procedure and nationwide homogeneous data, which facilitates a comparison
740 between catchments. The methodology is flexible and can be adapted to other regions outside
741 Switzerland if recruitment processes (especially with regard to SilvaProtect-CH trajectories) were
742 modelled with more generic approaches.

743 The two models presented here correspond to a hazard index mapping in terms of
744 processing depth and degree of detail for a hazard assessment. The geospatial modelling results
745 indicate areas of potential LW recruitment, however without precise information about the
746 intensities occurring. In contrast, the estimated LW supply for the large scenario is based on the
747 data of events with a return period of approximately 50 to 150 years. The approach presented here
748 is a useful tool to give a comprehensive overview and direct attention to areas where a more
749 precise assessment of the LW situation is probably useful, for example in connection with an
750 estimation of sediment loads in torrents.

751



752 6 CONCLUSIONS

753 Two GIS-based models are presented in this contribution to identify large wood (LW)
754 sources and to estimate LW supply to rivers. Both models, called empirical GIS approach (EGA)
755 and Fuzzy-Logic GIS approach (FGA), consider landslides, debris flows, bank erosion, and
756 mobilization of instream wood as recruitment processes. The results are volumetric estimates of
757 LW supply based on three different scenarios of process frequency and magnitude. Results of
758 model applications to 40 Swiss catchments were used to compare both the two models with each
759 other and the performance in relation to observed (empirical) LW volumes. Further, a literature
760 review of existing LW supply models proposed in the last 35 years was conducted, set into context
761 and remaining challenges were identified.

762 EGA shows significantly higher values for potential LW supply. However, after reducing
763 the potential volume with different methods, estimated LW supply volumes are in the same order
764 of magnitude for both models, with FGA showing generally somewhat larger values. In case of
765 EGA, landslides are the dominant recruitment process, whereas bank erosion is dominant for
766 FGA. Both models show under- and overestimation of observed wood volumes V_{obs} , with more
767 tendency for overestimation. Overestimation stays generally within two orders of magnitude
768 (typically larger values for FGA), underestimation within one order of magnitude (typically
769 smaller values for EGA).

770 The modelling and quantification of wood supply volumes is characterised by many
771 uncertainties. After all, the two models presented in this study allow quantifying the magnitude
772 of the expected LW supply, thus further expert judgement and knowledge of local (geomorphic)
773 characteristics is required to adequately interpret such results. LW supply modelling can be
774 further improved by integrating more physically-based and/or probabilistic inputs for the spatial
775 identification of recruitment processes. Likewise, the parametrization and validation of LW
776 supply models remain complex. Post flood event analysis provide valuable empirical datasets that
777 can be used to validate results and further develop LW supply models that can be useful for hazard
778 assessment, infrastructure design, and the definition of management strategies.



779 **ACKNOWLEDGEMENTS**

780 We thank the Swiss Federal Office for the Environment (FOEN) for funding the research
781 program "Large Wood Management in Rivers" (WoodFlow research program; contract no.
782 15.0018.PJ/O192-3154).

783 Special thanks go to Peter Waldner (WSL) for providing valuable empirical data from flood
784 events; Benjamin Kuratli (formerly University of Zurich) for helping to develop earlier versions
785 of the EGA; Bronwyn Price, Christian Ginzler and Markus Huber (all WSL) for providing data
786 from the Swiss National Forest Inventory; and finally, Stéphane Losey (FOEN) for providing all
787 the required SilvaProtect-CH data.

788



789 **REFERENCES**

790 Bachmann Walker, A. 2012. Ausmass und Auftreten von Seitenerosionen bei Hochwasser.
791 Auswertung von hydraulisch verursachten Seitenerosionen und Herleitung von empirischen
792 Zusammenhängen zur Ermittlung des Erosionsausmasses und -auftreten. Master thesis.
793 Geographisches Institut der Universität Bern (in German).

794 Beechie TJ, Pess G, Kennard P, Bilby RE, Bolton S. 2000. Modeling Recovery Rates and
795 Pathways for Woody Debris Recruitment in Northwestern Washington Streams. *North American*
796 *Journal of Fisheries Management* 20 : 436–452. DOI: 10.1577/1548-
797 8675(2000)020<0436:mrrapf>2.3.co;2

798 Benda LE, Litschert SE, Reeves G, Pabst R. 2016. Thinning and in-stream wood recruitment
799 in riparian second growth forests in coastal Oregon and the use of buffers and tree tipping as
800 mitigation. *Journal of Forestry Research* 27 : 821–836. DOI: 10.1007/s11676-015-0173-2

801 Benda L, Bigelow P. 2014. On the patterns and processes of wood in northern California
802 streams. *Geomorphology* 209 : 79–97. DOI: 10.1016/j.geomorph.2013.11.028

803 Benda L, Miller D, Andras K, Bigelow P, Reeves G, Michael D. 2007. NetMap: A new tool
804 in support of watershed science and resource management. *Forest Science* 53 : 206–219. DOI:
805 10.1093/forestscience/53.2.206

806 Benda LE, Sias JC. 2003. A quantitative framework for evaluating the mass balance of in-
807 stream organic debris. *Forest Ecology and Management* 172 : 1–16. DOI: 10.1016/S0378-
808 1127(01)00576-X

809 Bezzola GR, Gantenbein S, Hollenstein R, Minor HE. 2002. Verklauung von
810 Brückenquerschnitten; Internationales Symposium Moderne Methoden und Konzepte im
811 Wasserbau; Mitteilung der Versuchsanstalt für Wasserbau, Hydrologie und Glaziologie der ETH
812 Zürich, Nr. 175

813 Blaschke T, Tiede D, Heurich M. 2004. 3D landscape metrics to modelling forest structure
814 and diversity based on laser scanning data. *International Archives of the Photogrammetry,*
815 *Remote Sensing and Spatial Information Sciences XXXVI-8W2* : 129–132.

816 Bonham-Carter GF, Agterberg FP, Wright DF. 1990. Weights of evidence modelling: a new
817 approach to mapping mineral potential. In *Statistical applications in the earth sciences*, Paper89-
818 9, Agterberg FP and Bonham-Carter G (eds). Canadian Government Publishing Centre: Ottawa,
819 Ontario, Canada; 171–183.

820 Bragg DC. 2000. Simulating catastrophic and individualistic large woody debris recruitment
821 for a small riparian system. *Ecology* 81 : 1383. DOI: 10.2307/177215



- 822 Braudrick CA, Grant GE, Ishikawa Y, Ikeda H. 1997. Dynamics of wood transport in
823 streams: A flume experiment. *Earth Surface Processes and Landforms* 22 : 669–683. DOI:
824 10.1002/(SICI)1096-9837(199707)22:7<669::AID-ESP740>3.3.CO;2-C
- 825 Cavalli M, Trevisani S, Comiti F, Marchi L. 2013. Geomorphometric assessment of spatial
826 sediment connectivity in small Alpine catchments. *Geomorphology* 188 : 31–41. DOI:
827 10.1016/j.geomorph.2012.05.007
- 828 Cislaghi A, Rigon E, Lenzi MA, Bischetti GB. 2018. A probabilistic multidimensional
829 approach to quantify large wood recruitment from hillslopes in mountainous-forested catchments.
830 *Geomorphology* 306 : 108–127. DOI: 10.1016/j.geomorph.2018.01.009
- 831 Comiti F, Lucía A, Rickenmann D. 2016. Large wood recruitment and transport during large
832 floods: A review. *Geomorphology* 269: 23–39. DOI: 10.1016/j.geomorph.2016.06.016
- 833 Dixon SJ. 2013. Investigating the effects of large wood and forest management on flood risk
834 and flood hydrology, University of Southampton
- 835 Dorren L. 2017. FINT – Find individual trees. User manual. ecorisQ paper.
- 836 Downs PW, Simon A. 2001. Fluvial geomorphological analysis of the recruitment of large
837 woody debris in the Yalobusha river network, Central Mississippi, USA. *Geomorphology* 37 :
838 65–91. DOI: 10.1016/S0169-555X(00)00063-5
- 839 Eaton BC, Hassan MA, Davidson SL. 2012. Modeling wood dynamics, jam formation, and
840 sediment storage in a gravel-bed stream. *Journal of Geophysical Research: Earth Surface* 117 :
841 1–18. DOI: 10.1029/2012JF002385
- 842 FOEN. 2019. Schwemmholz in Fließgewässern. Ein praxisorientiertes Forschungsprojekt.
843 Bundesamt für Umwelt, Bern. Umwelt-Wissen Nr. 1910, 100 p.
- 844 FOEN. 2015. Einzugsgebietgliederung Schweiz, EZGG-CH. Bundesamt für Umwelt, Bern.
845 <http://www.bafu.admin.ch/ezgg-ch>
- 846 Franceschi S, Antonello A, Crema S, Comiti F. 2019. GIS-based approach to assess large
847 wood transport in mountain rivers during floods. Preprint DOI: 10.13140/RG.2.2.31787.08480
- 848 Gasser E, Perona P, Dorren L, Phillips C, Hübl J, Schwarz M. 2020. A new framework to
849 model hydraulic bank erosion considering the effects of roots. *Water (Switzerland)* 12 DOI:
850 10.3390/w12030893
- 851 Gasser E, Schwarz M, Simon A, Perona P, Phillips C, Hübl J, Dorren L. 2019. A review of
852 modeling the effects of vegetation on large wood recruitment processes in mountain catchments.
853 *Earth-Science Reviews* 194 : 350–373. DOI: 10.1016/j.earscirev.2019.04.013



- 854 Gasser E, Simon A, Perona P, Dorren L, Hübl J, Schwarz M. 2018. Quantification of
855 potential recruitment of large woody debris in mountain catchments considering the effects of
856 vegetation on hydraulic and geotechnical bank erosion and shallow landslides. Paquier A and
857 Rivière N (eds). E3S Web of Conferences 40 DOI: 10.1051/e3sconf/20184002046
- 858 Ginzler C, Price B, Bösch R, Fischer C, Hobi ML, Psomas A, Rehush N, Wang Z, Waser
859 LT. 2019. Area-Wide Products. In Swiss National Forest Inventory – Methods and Models of the
860 Fourth Assessment, Fischer C and Traub B (eds). Springer International Publishing: Cham; 125–
861 142.
- 862 von Glutz M. 2011. Verfahren zur Abschätzung des Schwemholzpotentials von
863 Wildbächen. Bachelor thesis. Schweizerische Hochschule für Landwirtschaft (SHL), Zollikofen,
864 Switzerland. 116 p. (in German)
- 865 Gregory SV, Meleason MA, Sobota DJ. 2003. Modeling the dynamics of wood in streams
866 and rivers. In American Fisheries Society Symposium 37, Gregory S V., Boyer K, and Gurnell
867 A (eds). 315–335.
- 868 Harmon ME, Franklin JF, Swanson FJ, Sollins P, Gregory SV, Lattin JD, Anderson NH,
869 Cline SP, Aumen NG, Sedell JR, Lienkaemper GW, Cromack K, Cummins KW. 1986. Ecology
870 of coarse woody debris in temperate ecosystems. In: MacFadyen, A.; Ford, E. D., eds. Advances
871 in ecological research. Orlando, FL: Academic Press, Inc.: 15: 133-302.
- 872 Hassan MA, Bird S, Reid D, Hogan D. 2016. Simulated wood budgets in two mountain
873 streams. *Geomorphology* 259 : 119–133. DOI: 10.1016/j.geomorph.2016.02.010
- 874 Hunziker G. 2017. Schwemholz Zulug. Untersuchungen zum Schwemholzaufkommen in
875 der Zulug und deren Seitenbächen. Hunziker Gefahrenmanagement Bericht (Gemeinde
876 Steffisburg).
- 877 Hunzinger L, Durrer S. 2008. Seitenerosion, in: Bezzola, G.R., Hegg, C. (Eds.),
878 Ereignisanalyse Hochwasser 2005, Teil 2 – Analyse von Prozessen, Massnahmen Und
879 Gefahregrundlagen. Umwelt-Wissen, Nr. 0825, Bundesamt für Umwelt BAFU & Eidg.
880 Forschungsanstalt WSL, Bern, pp. 125-136 (in German).
- 881 Hupp CR, Simon A. 1991. Bank accretion and development of vegetated depositional
882 surfaces along modified alluvial channels, *Geomorphology*, 4, 111-124.
- 883 Kasprak A, Magilligan FJ, Nislow KH, Snyder NP. 2012. A LIDAR-derived evaluation of
884 watershed-scale large woody debris sources and recruitment mechanisms: Coastal Maine, USA.
885 *River Research and Applications* 28 : 1462–1476. DOI: 10.1002/rra.1532
- 886 Kennard P, Pess G, Beechie T, Bilby R, Berg D. 1999. Riparian-in-a-box: A manager's tool



- 887 to predict the impacts of riparian management on fish habitat. In Forest–Fish Conference: Land
888 Management Practices Affecting Aquatic Ecosystems. Natural Resources Canada, Canadian
889 Forest Service Information Report NOR-X-356. , Brewin M and Monit D (eds). Calgary, Alberta,
890 Canada; 483–490.
- 891 Lassetre NS, Kondolf GM. 2012. Large woody debris in urban stream channels: Redefining
892 the problem. *River Research and Applications* 28 : 1477–1487. DOI: 10.1002/rra.1538
- 893 Losey S, Wehrli A. 2013. Schutzwald in der Schweiz. Vom Projekt SilvaProtect-CH zum
894 harmonisierten Schutzwald . Bern, Schweiz
- 895 Lucía A, Andrea A, Daniela C, Marco C, Stefano C, Silvia F, Enrico M, Martin N, Stefan S,
896 Francesco C. 2015a. Monitoring and Modeling Large Wood Recruitment and Transport in a
897 Mountain Basin of North-Eastern Italy. In *Engineering Geology for Society and Territory -*
898 *Volume 3*. Springer International Publishing: Cham; 155–158.
- 899 Lucía A, Comiti F, Borga M, Cavalli M, Marchi L. 2015b. Dynamics of large wood during
900 a flash flood in two mountain catchments. *Natural Hazards and Earth System Sciences* 15 : 1741–
901 1755. DOI: 10.5194/nhess-15-1741-2015
- 902 Lucía A, Schwientek M, Eberle J, Zarfl C. 2018. Planform changes and large wood dynamics
903 in two torrents during a severe flash flood in Braunsbach, Germany 2016. *Science of the Total*
904 *Environment* 640–641 : 315–326. DOI: 10.1016/j.scitotenv.2018.05.186
- 905 Malanson GP, Kupfer JA. 1993. Simulated fate of leaf litter and large woody debris at a
906 riparian cutbank. *Canadian Journal of Forest Research* 23 : 582–590.
- 907 Martin D, Benda L. 2001. Patterns of in-stream wood recruitment and transport at the
908 watershed scale. In *Transactions of the American Fisheries Society* 130 , . 940–958.
- 909 Mazzorana B, Hübl J, Zischg A, Largiader A. 2011. Modelling woody material transport and
910 deposition in alpine rivers. *Natural Hazards* 56 : 425–449. DOI: 10.1007/s11069-009-9492-y
- 911 Mazzorana B, Zischg A, Largiader A, Hübl J. 2009. Hazard index maps for woody material
912 recruitment and transport in alpine catchments. *Natural Hazards and Earth System Science* 9 :
913 197–209. DOI: 10.5194/nhess-9-197-2009
- 914 Meleason MA, Gregory S V., Bolte JP. 2003. Implications of riparian management strategies
915 on wood in streams of the Pacific northwest. *Ecological Applications* 13 : 1212–1221. DOI:
916 10.1890/02-5004
- 917 Minor KP. 1997. Estimating large woody debris recruitment from adjacent riparian areas,
918 Oregon State University, Corvallis, Oregon, USA



- 919 Montgomery DR, Dietrich WE. 1994. A physically based model for the topographic control
920 on shallow landsliding. *Water Resources Research* 30 : 1153–1171. DOI: 10.1029/93WR02979
- 921 Montgomery DR, Piégay H. 2003. Wood in rivers: interactions with channel morphology
922 and processes. *Geomorphology* 51 : 1–5. DOI: 10.1016/S0169-555X(02)00322-7
- 923 Murphy ML, Koski K V. 1989. Input and Depletion of Woody Debris in Alaska Streams and
924 Implications for Streamside Management. *North American Journal of Fisheries Management* 9 :
925 427–436. DOI: 10.1577/1548-8675(1989)009<0427:iadowd>2.3.co;2
- 926 Piégay H, Thévenet A, Citterio A. 1999. Input, storage and distribution of large woody debris
927 along a mountain river continuum, the Drôme River, France. *CATENA* 35 : 19–39. DOI:
928 10.1016/S0341-8162(98)00120-9
- 929 R Core Team. 2019. R: A Language and Environment for Statistical Computing. R
930 Foundation for Statistical Computing, Vienna, Austria. <https://www.R-project.org/>
- 931 Rainville RC, Rainville SC, Linder EL. 1986. Riparian silvicultural strategies for fish habitat
932 emphasis. 186–196 pp.
- 933 Rickenmann D. 1997. Schwemmholz und Hochwasser. *Wasser, Energie, Luft* 89 : 115-119
934 (in German).
- 935 Rickenmann, D., Canuto, N., Koschni, A. 2008. Ereignisanalyse Hochwasser 2005.
936 Teilprojekt Vertiefung Wildbäche: Einfluss von Lithologie/Geotechnik und Niederschlag auf die
937 Wildbachaktivität beim Hochwasser 2005. Birmensdorf, Switzerland.
- 938 Rickenmann, D., Koschni, A. 2010. Sediment loads due to fluvial transport and debris flows
939 during the 2005 flood events in Switzerland. *Hydrol. Process.* 24, 993–1007.
940 doi:10.1002/hyp.7536
- 941 Rickenmann D, Badoux A, Hunzinger L. 2016. Significance of sediment transport processes
942 during piedmont floods: the 2005 flood events in Switzerland. *Earth Surface Processes and*
943 *Landforms* 41 : 224–230. DOI: 10.1002/esp.3835
- 944 Rickli C, Badoux A, Rickenmann D, Steeb N, Waldner P. 2018. Large wood potential, piece
945 characteristics, and flood effects in Swiss mountain streams. *Physical Geography* 3646 : 1–23.
946 DOI: 10.1080/02723646.2018.1456310
- 947 Rickli, C., McArdeLL, B., Badoux, A., Loup, B., 2016. Database shallow landslides and
948 hillslope debris flows, in: Kobltschnig, G. (Ed.), 13th Congress INTERPRAEVENT 2016. 30
949 May to 2 June 2016. Lucerne, Switzerland. International Research Society INTERPRAEVENT,
950 Klagenfurt, Austria, pp. 242–243.



- 951 Rickli C, Bucher H. 2006. Einfluss ufernaher Bestockungen auf das
952 Schwemmholtzvorkommen in Wildbächen . Eidg. Forschungsanstalt für Wald Schnee und
953 Landschaft WSL: Birmensdorf, 94 pp. (in German)
- 954 Rigon E, Comiti F, Lenzi MA. 2012. Large wood storage in streams of the Eastern Italian
955 Alps and the relevance of hillslope processes. *Water Resources Research* 48 : 1–18. DOI:
956 10.1029/2010WR009854
- 957 Rimböck A. 2001. Luftbildbasierte Abschätzung des Schwemmholtzpotentials (LASP) in
958 Wildbächen. In: Festschrift aus Anlass des 75-jährigen Bestehens der Versuchsanstalt für
959 Wasserbau und Wasserwirtschaft der Technischen Universität München in Obernach
- 960 Rimböck A. 2003. Schwemmholtzrückhalt in Wildbächen: Grundlagen zu Planung und
961 Berechnung von Seilnetzsperrern . Ausgabe 94. Lehrstuhl und Versuchsanstalt für Wasserbau und
962 Wasserwirtschaft der Technischen Universität München
- 963 Ruiz-Villanueva V, Mazzorana B, Bladé E, Bürkli L, Iribarren-Anacona P, Mao L,
964 Nakamura F, Ravazzolo D, Rickenmann D, Sanz-Ramos M, Stoffel M, Wohl E. 2019.
965 Characterization of wood-laden flows in rivers. *Earth Surface Processes and Landforms*.
966 <https://doi.org/https://doi.org/10.1002/esp.4603>
- 967 Ruiz-Villanueva V, Bladé Castellet E, Díez-Herrero A, Bodoque JM, Sánchez-Juny M.
968 2014a. Two-dimensional modelling of large wood transport during flash floods. *Earth Surface*
969 *Processes and Landforms* 39 : 438–449. DOI: 10.1002/esp.3456
- 970 Ruiz-Villanueva V, Bladé E, Sánchez-Juny M, Marti-Cardona B, Díez-Herrero A, Bodoque
971 JM. 2014b. Two-dimensional numerical modeling of wood transport. *Journal of*
972 *Hydroinformatics* 16 : 1077. DOI: 10.2166/hydro.2014.026
- 973 Ruiz-Villanueva V, Díez-Herrero A, Ballesteros JA, Bodoque JM. 2014c. Potential large
974 woody debris recruitment due to landslides, bank erosion and floods in mountain basins: a
975 quantitative estimation approach. *River Research and Applications* 30 : 81–97. DOI:
976 10.1002/rra.2614
- 977 Ruiz-Villanueva V, Piégay H, Gurnell AM, Marston RA, Stoffel M. 2016. Recent advances
978 quantifying the large wood dynamics in river basins: New methods and remaining challenges.
979 *Reviews of Geophysics* 54 : 611–652. DOI: 10.1002/2015RG000514
- 980 Ruiz-Villanueva V, Stoffel M. 2018. Application of fuzzy logic to large organic matter
981 recruitment in forested river basins. *Proceedings of the 5th IAHR Europe Congress —New*
982 *Challenges in Hydraulic Research and Engineering* : 467–468. DOI: 10.3850/978-981-11-2731-
983 1_047-cd



- 984 Ruiz-Villanueva V, Wyzga B, Zawiejska J, Hajdukiewicz M, Stoffel M. 2015. Factors
985 controlling large-wood transport in a mountain river. *Geomorphology* DOI:
986 10.1016/j.geomorph.2015.04.004
- 987 Ruiz-Villanueva V, Bodoque JM, Díez-Herrero A, Eguibar MA, Pardo-Igúzquiza E. 2013.
988 Reconstruction of a flash flood with large wood transport and its influence on hazard patterns in
989 an ungauged mountain basin. *Hydrological Processes* 27 : 3424–3437. DOI: 10.1002/hyp.9433
- 990 Ruiz-Villanueva V, Gamberini C, Bladé E, Stoffel M, Bertoldi W. 2020. Numerical
991 Modeling of Instream Wood Transport, Deposition, and Accumulation in Braided Morphologies
992 Under Unsteady Conditions: Sensitivity and High-Resolution Quantitative Model Validation.
993 *Water Resources Research* 56 : 1–22. DOI: 10.1029/2019WR026221
- 994 Ruiz-Villanueva V, Badoux A, Rickenmann D, Böckli M, Schläfli S, Steeb N, Stoffel M,
995 Rickli C. 2018. Impacts of a large flood along a mountain river basin: the importance of channel
996 widening and estimating the large wood budget in the upper Emme River (Switzerland). *Earth
997 Surface Dynamics*, June, 1–42. <https://doi.org/https://doi.org/10.5194/esurf-6-1115-2018>
- 998 RStudio Team. 2021. RStudio: Integrated Development Environment for R. RStudio, PBC,
999 Boston, MA URL <http://www.rstudio.com/>
- 1000 Simon A. 1989. Shear-strength determination and stream-bank instabil- ity in loess-derived
1001 alluvium, West Tennessee, USA, in *Applied Quaternary Research*, edited by E. J. DeMulder and
1002 B. P. Hageman, pp. 129-146, A. A. Balkema Publications, Rotterdam.
- 1003 Schalko I. 2019. Laboratory Flume Experiments on the Formation of Spanwise Large Wood
1004 Accumulations : I. Effect on Backwater Rise *Water Resources Research*. DOI:
1005 10.1029/2018WR024649
- 1006 Schalko I, Schmocker L, Weitbrecht V, Boes RM. 2018. Backwater Rise due to Large Wood
1007 Accumulations. *Journal of Hydraulic Engineering* 144 : 04018056. DOI:
1008 10.1061/(ASCE)HY.1943-7900.0001501
- 1009 Schloerke B, Cook D, Larmarange J, Briatte F, Marbach M, Thoen E, Elberg A, Crowley J.
1010 2021. GGally: Extension to 'ggplot2'. R package version 2.1.2. [https://CRAN.R-
1011 project.org/package=GGally](https://CRAN.R-project.org/package=GGally)
- 1012 Schmocker L, Weitbrecht V. 2013. Driftwood : Risk Analysis and Engineering Measures.
1013 *Journal of Hydraulic Engineering* 139 : 683–695. DOI: 10.1061/(ASCE)HY.1943-7900.0000728.
- 1014 Seo J, Nakamura F, Chun KW. 2010. Dynamics of large wood at the watershed scale: A
1015 perspective on current research limits and future directions. *Landscape and Ecological
1016 Engineering* 6 : 271–287. DOI: 10.1007/s11355-010-0106-3



- 1017 Van Sickle J, Gregory S V. 1990. Modeling inputs of large woody debris to streams from
1018 falling trees. *Canadian Journal of Forest Research* 20 : 1593–1601. DOI: 10.1139/x90-211
- 1019 Spreitzer G, Tunncliffe J, Friedrich H. 2020. Porosity and volume assessments of large wood
1020 (LW) accumulations. *Geomorphology* 358 : 107122. DOI: 10.1016/j.geomorph.2020.107122
- 1021 Steeb N. 2018. Empirical prediction of large wood transport during flood events. 5th IHAR
1022 Europe Congress. New challenges in Hydraulic Research and Engineering. Trento, Italy.
- 1023 Steeb N, Badoux A, Rickli C, Rickenmann D. 2022. Empirical prediction of large wood
1024 transport during flood events. 11th IHAR International Conference on Fluvial Hydraulics, River
1025 Flow 2022. Kingston and Ottawa, November 8-10, 2022.
- 1026 Steeb N, Badoux A, Rickli C, Rickenmann D. 2019a. Detailbericht zum Forschungsprojekt
1027 WoodFlow: Empirische Schätzformeln. Birmensdorf
- 1028 Steeb N, Badoux A, Rickli C, Rickenmann D. 2019b. Detailbericht zum Forschungsprojekt
1029 WoodFlow: Empirischer GIS-Ansatz. Birmensdorf
- 1030 Steeb N, Kuratli B, Rickli C, Badoux A, Rickenmann D. 2017a. GIS-Modellierung des
1031 Schwemmholtzpotentials in alpinen Einzugsgebieten. *Agenda FAN 2/2017 2* : 9–12.
- 1032 Steeb N, Rickenmann D, Badoux A, Rickli C, Waldner P. 2017b. Large wood recruitment
1033 processes and transported volumes in Swiss mountain streams during the extreme flood of August
1034 2005. *Geomorphology* 279 : 112–127. DOI: <https://doi.org/10.1016/j.geomorph.2016.10.011>
- 1035 Steel EA, Richards WH, Kelsley KA. 2003. Wood and wildlife: Benefits of river wood to
1036 terrestrial and aquatic vertebrates. In *The ecology and Management of Wood in World Rivers*.
1037 *American Fisheries Society Symposium* 37 , Gregory S, Boyer K, and Gurnell A (eds). 235–247.
- 1038 Strahler AN. 1957. Quantitative analysis of watershed geomorphology. *Eos, Transactions*
1039 *American Geophysical Union* 38 : 913–920. DOI: 10.1029/TR038i006p00913
- 1040 Thevenet A, Citterio A, Piegay H. 1998. A new methodology for the assessment of large
1041 woody debris accumulations on highly modified rivers (example of two French Piedmont rivers).
1042 *Regulated Rivers: Research & Management* 14 : 467–483. DOI: 10.1002/(SICI)1099-
1043 1646(199811)14:6<467::AID-RRR514>3.0.CO;2-X
- 1044 Uchiogi T, Shima J, Tajima H, Ishikawa Y. 1996. Design Methods for Wood-Debris
1045 Entrapment. 279–288 pp.
- 1046 Waldner P et al. 2009. Schwemmholtz des Hochwassers 2005. Schlussbericht des WSL-
1047 Teilprojekts Schwemmholtz der Ereignisanalyse BAFU/WSL des Hochwassers 2005. .
1048 Birmensdorf, 70 pp. (in German)



- 1049 Welty JJ, Beechie T, Sullivan K, Hyink DM, Bilby RE, Andrus C, Pess G. 2002. Riparian
1050 aquatic interaction simulator (RAIS): A model of riparian forest dynamics for the generation of
1051 large woody debris and shade. *Forest Ecology and Management* 162: 299–318. DOI:
1052 10.1016/S0378-1127(01)00524-2
- 1053 Wohl E, Scott DN. 2016. Wood and sediment storage and dynamics in river corridors. *Earth*
1054 *Surface Processes and Landforms* : n/a-n/a. DOI: 10.1002/esp.3909
- 1055 Wohl E. 2017. Bridging the gaps: An overview of wood across time and space in diverse
1056 rivers. *Geomorphology*, 279, 3–26. <https://doi.org/10.1016/j.geomorph.2016.04.014>
- 1057 Wondzell SM, Bisson PA. 2003. Influence of wood on aquatic biodiversity. In *The ecology*
1058 *and Management of Wood in World Rivers*. American Fisheries Society Symposium 37 , Gregory
1059 S, Boyer K, and Gurnell A (eds). Bethesda, Maryland; 249–263.
- 1060 WSL. 2016. Schweizerisches Landesforstinventar LFI. Daten der Erhebungen 2004/06
1061 (LFI3) und 2009/13 (LFI4). Markus Huber 06.06.2016.
- 1062 Zeh Weissmann H, Könitzer C, Bertiller A. 2009. Strukturen der Fließgewässer in der
1063 Schweiz. Zustand von Sohle, Ufer und Umland (Ökomorphologie); Ergebnisse der
1064 ökomorphologischen Kartierung. Umwelt-Zustand Nr. 0926 . Bern
- 1065 Zischg AP, Galatioto N, Deplazes S, Weingartner R, Mazzorana B. 2018. Modelling
1066 spatiotemporal dynamics of large wood recruitment, transport, and deposition at the river reach
1067 scale during extreme floods. *Water (Switzerland)* 10 : 1134. DOI: 10.3390/w10091134